# Phase Equilibria in the Al-Ti-Cr System During Solidification

Kostyantyn Korniyenko[1] · Konstantin Meleshevich[1] · Anatoliy Samelyuk[1] ·
Viktor Sobolev[2] · Lyudmila Kriklya[1]

**Abstract** Phase equilibria during solidification in the Al-Ti-Cr system in the compositional range from 40 to 100 at.% Al were studied using optical microscopy, scanning electron microscopy, electron probe microanalysis, differential thermal analysis, and x-ray diffraction. Specified solidus and liquidus surfaces, a melting diagram as their superposition, a Scheil diagram for solidification as well as series of isopleths were constructed. Continuous series of solid solutions between βTi and chromium, solid solutions based on αTi, TiAl, $Ti_{2+x}Al_{5-x}$, $TiAl_3$ (high- and room-temperature modifications), $Cr_5Al_8$ ($\gamma_3$, $\gamma_2$ and $\gamma_1$ phases), $CrAl_4$, $Cr_2Al_{11}$, $CrAl_7$ binary compounds and the ternary compound τ take part in phase equilibria. Thirteen invariant four-phase reactions (9—liquid transition, 3—peritectic, 1—eutectic) and three invariant three-phase (two peritectic and one eutectic maxima on monovariant curves) reactions involving liquid take place in the system. Isopleths at 50 at.%, 60 at.%, and 70 at.% Al demonstrate peculiarities of the phase diagram.

**Keywords** Al-Ti-Cr · isopleth · liquidus surface · phase equilibria · solidus surface

✉ Kostyantyn Korniyenko
korniyenkok@ukr.net

1 Frantsevich Institute for Problems of Materials Science, NASU, Kiev 03680, Ukraine

2 Technical Centre of National Academy of Sciences, Kiev 04070, Ukraine

## 1 Introduction

Titanium aluminides based on $\alpha_2$ ($Ti_3Al$), γ (TiAl) and $TiAl_3$ phases are currently being considered as candidate materials for elevated temperature applications due to their low densities, high-temperature strength as well as creep and oxidation resistance.[1-7] Alloys of ternary aluminum systems with titanium and *d* metals of the VI-VIII groups are promising for practical application in various fields of modern technology. Addition of a third alloying element, such as chromium, can improve the low temperature ductility[8] and the oxidation resistance.[9-12] To develop high-temperature structural and functional materials based on the titanium aluminides alloyed with chromium, an understanding of the phase equilibria in this system is essential.

Experimental investigations of phase equilibria during solidification in the ternary Al-Ti-Cr system were performed by several authors.[13-21] Liquidus isotherms in the Ti-rich corner (60-100 mass% Ti) were presented by Kornilov et al.[13] based on differential thermal analysis (DTA) results. Jewett et al.[14] studied the solubility of Cr in the TiAl phase at 1000 °C and 800 °C, and combined their own data with literature information to construct isothermal sections of the Al-Ti-Cr system at these temperatures over the whole range of compositions. In the Al-rich corner equilibria with participation of liquid phase are represented schematically. Mabuchi et al.[15] constructed the partial vertical section for 25 at.% Ti and between 5 and 30 at.% Cr. Below the solidus the ternary τ, $TiCr_{0.33}Al_{2.67}$ phase is in equilibrium with the $MgZn_2$-type Laves phase ($\gamma TiCr_2$). A tentative liquidus surface based on the investigation of the solidification structures of three alloy compositions, namely 40Al-50Ti-10Cr, 50Al-40Ti-10Cr and 52Al-28Ti-20Cr (at.%) was presented by Shao and

Tsakiropoulos.[16] Ichimaru et al.[17] focused on the investigation of the solidification behavior of alloys between 45 and 75 at.% Al using DTA. The partial liquidus surface with isothermal lines (1250-1370 °C) in the primary crystallization field of the ternary τ phase and the partial vertical section at 25 at.% Ti for between 5 and 30 at.% Cr were presented. Interpretation of the obtained results for equilibria with the liquid phase along this section differed from the interpretation of Mabuchi et al.[15]—according to the data of,[17] three-phase equilibrium with the liquid phase L + τ + (Cr) was shown, and the determined liquidus temperatures are slightly lower than the temperatures presented by Mabuchi et al.[15] Microstructural investigations of the Al-Ti-Cr system were performed by Barabash et al., [18] who described the position of the monovariant curve L + τ + (Cr) on the liquidus surface and proved the eutectic character of the corresponding reaction. The experimental results of Ichimaru et al.[17] were used by Mori and Ogi[19] to develop a progressive-type solidification equation for prediction of the second phase in solidification structures of alloys. Chen et al.[20] determined solid-state phase equilibria at 900 °C for up to 75 at.% Al and at 600 °C in the Al-rich corner (> 75 at.% Al). A reaction scheme linking these solid-state equilibria with the liquidus surface was presented. The liquidus surface for the region with up to 50 at.% aluminum is dominated by the primary crystallization field of a continuous series of solid solutions β (Ti, Cr, Al) with the body-centered cubic structure. In the Al-rich corner, the existence of the ternary invariant equilibrium $L_{pmax}$ + TiAl ↔ τ at 1393 °C was established, and with the addition of chromium, the binary peritectic L + αTi ↔ TiAl changes into an eutectic L ↔ αTi + TiAl. This eutectic valley descends monotonously through a series of transition reactions and ternary peritectics to end in the binary eutectic l ↔ $Cr_7Al_{45}$ (or $CrAl_7$) + (Al). Two vertical sections, namely $TiAl_3$-$CrAl_7$ and the section with atomic ratio Cr: Ti = 3: 1 were presented by Rusnyak et al.[21] These vertical sections show extended primary crystallization fields of the binary Al-Cr phases, which leads to a reduced $TiAl_3$ primary crystallization phase field. Thus, the L + $TiAl_3$ two-phase region shown in the $TiAl_3$-$CrAl_7$ vertical section of Rusnyak et al.,[21] extends only up to 5 at.% Cr, whereas in the work of Chen et al.[20] the primary crystallization field of the $TiAl_3$ phase extends almost up to the binary Al-Cr system (approximately to 10 at.% Cr).

On the basis of the above-listed experimental data, critical evaluations on the phase equilibria character in the Al-Ti-Cr system were carried out by Hayes,[22] Raghavan[23–25] and Bochvar et al.[26] In these reviews liquidus surfaces, various complete and partial isothermal sections in the temperature range 497-1200 °C, and reaction schemes were presented. Thermodynamic descriptions of

the ternary Al-Ti-Cr system[27-30] have been developed in the early 2010s on the basis of extensive literature reviews of available information about phase equilibria. However, the construction of the solidus projection as well as the analysis of the phase equilibria just below the solidus temperatures for Al contents < 75 at.% was not presented then.

This investigation was carried out to eliminate this information gap. The results obtained were published.[31] The melting behavior of the Al-Ti-Cr alloys in the compositional range between 45 and 75 at.% Al was experimentally studied. The primary crystallization fields of the components and intermediate phases were determined based on the investigations of as-cast alloys using complementary experimental methods. Subsolidus annealing in the temperature range between 1000 and 1250 °C was performed to determine the three-phase equilibria of solid phases corresponding to the solidus surface. Temperatures of the invariant reactions were measured using DTA experiments of annealed samples. To assess the invariant reactions, alloys located inside the various reaction planes were prepared, annealed below the reaction temperatures and characterized using complementary experimental methods. Based on subsolidus annealing experiments, the solidus surface was constructed for the first time. Also the Scheil reaction scheme for the Al-Ti-Cr system involving the liquid phase was constructed. Based on literature data, in particular, Kriegel et al.,[31] and few selected experiments in the vicinity of the TiAl phase compositions, a new thermodynamic description of the ternary Al-Ti-Cr system by the CALPHAD method was proposed by Witusiewicz et al.[32] The elaborate thermodynamic description was applied to calculate selected phase equilibria to provide a comparison between calculated and experimental results. The calculations reproduced the experimental data of various authors reasonably well. The phase equilibria proposed by Witusiewicz et al.,[32] at some points differs quite significantly this group's data.[31] In particular, significantly different positions of the three-phase fields (αTi) + (βTi, Cr) + γ, γ + τ + (βTi, Cr), τ + (βTi, Cr) + $γ_3$ and τ + $γ_3$ + ε on the solidus surface; homogeneity ranges of (βTi, Cr) and (αTi); temperature of invariant equilibria with participation of liquid, (αTi), (βTi, Cr) and γ; character of invariant equilibria with participation of liquid and the $γ_3$, ε and μ phases etc.

To resolve the existing contradictions about phase equilibria in the crystallization of alloys, key experiments were performed on an additional series of alloy samples in as-cast and annealed at subsolidus temperatures states. From these results, specified solidus and liquidus surfaces, a melting diagram, a Scheil diagram for solidification as well as series of isopleths of the ternary system Al-Ti-Cr in

J. Phase Equilib. Diffus. (2022) 43:427–447

429

the range of compositions 40-100 at.% Al were constructed.

## 2 Binary Systems

The thermodynamic description of the Al-Ti binary system was obtained by Witusiewicz et al.[33] by modeling the Gibbs energy of all individual phases using the CALPHAD approach. The model parameters have been evaluated by means of the computer optimization module PARROT, available within Thermo-Calc, taking into account recent experimental data and critically assessed information on phase equilibria and thermodynamic properties. The calculations results were in close agreement with the experimental data on both phase equilibria and thermodynamics in the entire Al-Ti system.

The Al-Cr phase diagram is accepted from the thermodynamic assessment of Witusiewicz et al.[32] carried out by using the CALPHAD technique using available literature data including some of their own key experimental data. Experimental data of Kurtuldu et al.[34] obtained in the planar front solidification experiments of Al-Cr alloys confirmed peritectic character of the phase equilibrium with the participation of the $CrAl_7$ phase and aluminium-based solid solutions[34] (according to the reaction $L + CrAl_7$ (or $Cr_7Al_{45}$[34]) $\leftrightarrow$ (Al) at 662 °C[32]). Cui et al.[35] attempted an experimental study (diffusion couples technique) and thermodynamic assessment of the binary Al-Cr and the ternary Al-Cr-Mg systems but their conclusions concerning phase equilibria in the Al-Cr system were contradictory and ignored the results of Witusiewicz et al.[32].

The Ti-Cr binary phase diagram is accepted from CALPHAD thermodynamic assessment of Cupid et al.[28]. Before this thermodynamic description there were contradictions in the literature regarding the presence of an intermediate temperature hexagonal C36 Laves phase polytype (the $\beta TiCr_2$ phase) in addition to the low temperature cubic C15 and the high temperature hexagonal C14 polytypes (the $\alpha TiCr_2$ and $\gamma TiCr_2$ phases respectively).[36] The description for the binary Ti-Cr system proposed by Cupid et al.[28] models all three modifications of the Laves phase whose homogeneity ranges are in very good agreement with the experimental data.[37-39]

Table 1 contains the data about crystal structure and the conditions of the existence of the solid phases that are formed in the ternary Al-Ti-Cr system and in the boundary binary systems. Only one ternary phase, namely the τ phase with composition $TiCr_{0.33}Al_{2.67}$, has been described.

## 3 Experimental Procedures

### 3.1 Sample Preparation

The starting materials were bulk aluminum (A-995 grade, 99.995%), iodide processed (crystal bar) titanium (99.8%) and refined metallic flake chromium (99.93%). Remelting of chromium and melting of twenty five Al-Ti-Cr samples was carried out by arc melting with a non-consumable tungsten electrode on a water-cooled copper hearth under argon (99.998%) purified by melting a titanium–zirconium getter for 5-6 min. The used arc-melting device was constructed in Department of physical chemistry of inorganic materials (Frantsevich Institute for Problems of Materials Science, NASU, Kyiv). The samples were remelted four to five times to attempt chemical homogeneity. The weight losses were no more than 0.7%, so the nominal compositions of the samples were accepted as representative. The samples, with a mass of about 4 g each, were solidified at cooling rate of about 100 K s$^{-1}$. Twenty two Al-Ti-Cr samples (Part 4) were subjected to homogenization heat treatment at about 50 °C below solidus (the solidus temperatures were previously determined by differential thermal analysis, Part 3.3) in an Ar (99.998%) atmosphere. The samples were placed in an $Al_2O_3$ crucible. After annealing, the samples were cooled within the furnace chamber.

### 3.2 Microstructure Analysis

Samples for microstructure analysis were prepared with a grinder and polisher machine. Grinding was carried out with SiC paper, followed by polishing with a water suspension of $Cr_2O_3$. The prepared samples were examined by optical microscopy (OM) and scanning electron microscopy (SEM) using a JEOL Superprobe-733 and JEOL Superprobe 8200 (JEOL, Tokyo, Japan) high-resolution scanning electron microscopes. Compositions of each phase and eutectic were determined using a JEOL Superprobe 8200 scanning electron microscope equipped with a wave-length dispersive spectroscopy system (WDX) for electron probe microanalysis (EPMA). A standard ZAF procedure was employed to adjust the measurements. Each composition was measured three to five times. The compositions of the samples measured by EPMA/WDS were compared with the nominal alloy compositions, and only slight deviations below 1 at.% were observed.

### 3.3 Differential Thermal Analysis

Differential thermal analysis (DTA) was carried out using a VDTA-7 technique (high-temperature differential thermal analyzer) with a W/W-20Re string thermocouple designed

**Table 1** Crystal structures of each phase in the Al-Ti-Cr ternary system

| System | Phase | Pearson's symbol | Space group | Prototype | Lattice parameters, nm | | | References |
|---|---|---|---|---|---|---|---|---|
| | | | | | $a$ | $b$ | $c$ | |
| Al-Ti | (Al) (a) | cF4 | $Fm\,\bar{3}\,m$ | Cu | 0.40496 | ... | ... | At 25 °C [40] |
| | $\varepsilon$, TiAl$_3$ (h) | tI8 | I4/mmm | TiAl$_3$ (h) | 0.3849 | ... | 0.8609 | 75 at.% Al, quenching from 1000 °C [41] |
| | TiAl$_3$ (r) | tI32 | I4/mmm | TiAl$_3$ (r) | 0.3877 | ... | 3.3828 | 76 at.% Al, quenching from 640 °C [41] |
| | $\zeta$, Ti$_{2+x}$Al$_{5-x}$ | tP28 | P4/mmm | Ti$_2$Al$_5$ | 0.39053 | ... | 2.91921 | (Ref 42) |
| | $\eta$, TiAl$_2$ | tI24 | I4$_1$/amd | HfGa$_2$ | 0.3970 | ... | 2.4309 | 66.7 at.% Al, quenching from 700 °C [41] |
| | Ti$_3$Al$_5$ | tP32 | P4/mbm | Ti$_3$Al$_5$ | 1.1293 | ... | 0.4038 | 62 at.% Al, quenching from 1100 °C [41] |
| | $\gamma$, TiAl | tP4 | P4/mmm | AuCu | 0.4000 | ... | 0.4075 | 50 at.% Al, quenching from 1000 °C [41] |
| | $\alpha_2$, Ti$_3$Al | hP8 | P6$_3$/mmc | Ni$_3$Sn | 0.5765 | ... | 0.4625 | 25 at.% Al [43] |
| | ($\beta$Ti) | cI2 | $Im\,\bar{3}\,m$ | W | 0.33065 | ... | ... | At 25 °C [40] |
| | ($\alpha$Ti) | hP2 | P6$_3$/mmc | Mg | 0.29506 | ... | 0.46835 | At 25 °C [40] |
| Al-Cr | $\theta$, CrAl$_7$ | mC104 | C2/m | V$_7$Al$_{45}$ | 2.5196 | 0.7574 β = 128.7° | 1.0949 | Quenching from 500 °C [44] |
| | $\eta$, Cr$_2$Al$_{11}$ | mP48 | P2 | CrAl$_5$ | 1.2880 | 0.7652 β = 122.2° | 1.0639 | (Ref 45) |
| | | ... | C2/c | ... | ~ 1.76 | ~ 3.05 β ≈ 90° | ~ 1.76 | (Ref 46) |
| | $\mu$, CrAl$_4$ | oC584 | Cmcm | ... | 1.24 | 3.46 | 2.02 | Quenching from 920 °C [47] |
| | | hP574 | P6$_3$/mmc | MnAl$_4$ | 2.01 | ... | 2.48 | (Ref 46) |
| | $\nu$, Cr$_4$Al$_{11}$ | aP15 | $P\,\bar{1}$ | Mn$_4$Al$_{11}$ | 0.5089 | 0.9033 | 0.5044 | (Ref 48) |
| | | | | | α = 91.84°, β = 100.77°, γ = 107.59° | | | |
| | $\gamma_3$, $\beta$Cr$_5$Al$_8$ (h$_2$) (b) | cI52 | $I\,\bar{4}\,3\,m$ | Cu$_5$Zn$_8$ | 0.909 | ... | ... | At 67.3 at.% Al [49] |
| | $\gamma_2$, $\gamma$Cr$_5$Al$_8$ (h$_1$) (b) | ... | ... | ... | ... | ... | ... | Rhombohedral representation [50] |
| | $\gamma_1$, $\alpha$Cr$_5$Al$_8$ (r) (b) | hR26 | $R\,\bar{3}\,m$ | Cr$_5$Al$_8$ | 0.78051 α = 109.217° | ... | ... | Hexagonal representation [51] |
| | | | | | 1.2909(2) | ... | 0.7840(1) | |
| | Cr$_2$Al | tI6 | I4/mmm | MoSi$_2$ | 0.3005 ÷ 0.3028 | ... | 0.8649 ÷ 0.8755 | At 25 °C to 853 °C [51] |
| Al-Cr | X | ... | ... | Cr$_5$Al$_3$ or Cr$_3$Al superlattice | ... | ... | ... | (Ref 32) |
| | (Cr) | cI2 | $Im\,\bar{3}\,m$ | W | 0.28848 | ... | ... | At 25 °C [40] |
| Ti-Cr | $\gamma$TiCr$_2$ (h$_2$) | hP12 | P6$_3$/mmc | MgZn$_2$ | 0.4908 | ... | 0.7965 | (Ref 52) |
| | $\beta$TiCr$_2$ (h$_1$) | hP24 | P6$_3$/mmc | MgNi$_2$ | 0.4884 | ... | 1.5854 | (Ref 53) |
| | $\alpha$TiCr$_2$ (r) | cF24 | $Fd\,\bar{3}\,m$ | MgCu$_2$ | 0.6943 | ... | ... | (Ref 54) |
| Al-Ti-Cr | $\tau$, TiCr$_{0.33}$Al$_{2.67}$ | cP4 | $Pm\,\bar{3}\,m$ | AuCu$_3$ | 0.3958 | ... | ... | (Ref 55) |

Parentheses in this table and elsewhere mean solid solution based on component or compound.

Different temperature modifications are indicated by lower case letters in parenthesis behind the phase designation, with: (h)—high temperature modification, (r)—room temperature modification. These letters are used in the sequence h$_2$, h$_1$, r.

by Kocherzhinskiy et al.[56,57]. The samples for DTA were placed in $Al_2O_3$ crucibles. The experiments were carried out on as-cast samples in a high purity (99.998%) helium atmosphere with heating and cooling rates of 40 °C·min$^{-1}$. To distinguish nearby thermal effects, lower heating/cooling rates of 5 °C min$^{-1}$ were also used. The accuracy of the temperature measurements was estimated to be ± 1%.

### 3.4 X-Ray Diffraction Analysis

XRD measurements were carried out in a DRON-3 diffractometer (Bourevestnik, Inc., St. Petersburg, Russia) on powder samples (fine powders were prepared by grinding in an agate mortar) or bulk samples for phase identification. The x-ray diffractograms of as-cast and annealed samples were recorded using Cu-K$_\alpha$ filtered radiation at an angular step of $2\theta = 0.05°$ and an exposure time of 2-8 s. The constituent phases were identified by comparison of experimental diffraction patterns with reference ones or patterns calculated using the Powder Cell software (version 2.4). The lattice parameters were calculated by least-squares refinement.

## 4 Results and Discussion

Phase equilibria in the Al-Ti-Cr system in the range of compositions 40-100 at.% Al during solidification are represented in this work by solidus and liquidus surfaces, a melting diagram as their compilation, a Scheil diagram for the solidification as well as isopleths at 50, 60 and 70 at.% Al. The majority of the obtained data confirmed the results of the works by Kriegel et al.[31] or Witusiewicz et al.[32] taking into account new valuable information on the phase constitution in the Al-Ti-Cr system.

### 4.1 Solidus Surface

The solidus surface projection of the Al-Ti-Cr system in the range of compositions 40-100 at.% Al (Fig. 1) was constructed based on the experimental data on the melting temperatures of alloys and their phase composition at subsolidus temperatures (Table 2, taking into account the results of studies of the alloys annealed at 1200 °C[31,58]) and considering lattice parameters of the phases according to the XRD measurements (Table 3).

On the solidus surface there is a continuous series of solid solutions between isostructural (cubic structure of W-type) β-titanium and chromium. The maximum solubility of aluminum in (βTi, Cr) reaches 46.4 at.% in the boundary binary system Al-Cr, and the position of its homogeneity range was established based on SEM and EPMA data of two-phase alloys #1 to #7 containing (βTi,
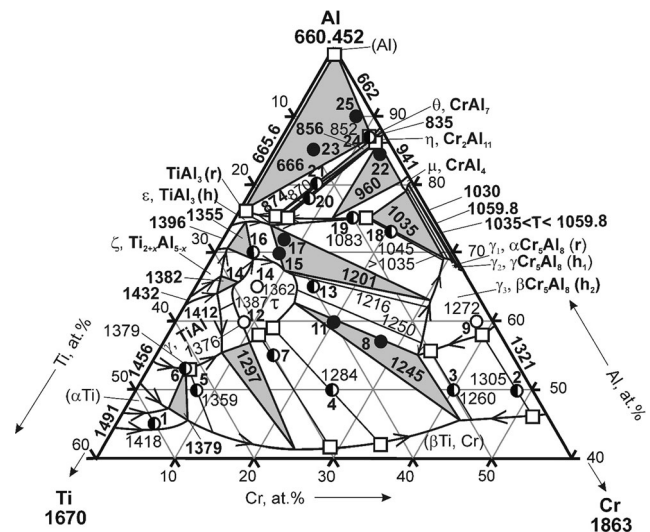


**Fig. 1** Solidus surface projection of the Al-Ti-Cr system in the range of compositions 40-100 at.% Al: open circle—single-phase sample; half vertical filled circle—two-phase sample; filled circle—three-phase sample; open square—EPMA data

Cr) (Table 2). The results obtained differed somewhat from the thermodynamic description of Witusiewicz et al.[32] and from the previous publication.[31] In particular, in the range of compositions near the section Ti: Cr = 1: 1 the solubility of aluminum is reduced to less than 42 at.% according to the alloys #4 and #7 annealed at subsolidus temperatures (Fig. 2a, b; Table 2). Microstructures of these alloys were in good agreement with the data of Kriegel et al.[58], which excluded the separation of the continuous (βTi, Cr) solid solution and the stability of the C14 Laves phase γTiCr$_2$ (h$_2$) shown by Chen et al.[27].

The value of the solubility of chromium in (αTi), about 6 at.%, at the temperature of the isothermal plane (αTi) + (βTi, Cr) + γ and the location of this plane is accepted according to the data of Witusiewicz et al.[32]. Position of the two-phase region (βTi, Cr) + (αTi) is specified compared to previous work,[31] using SEM and EPMA data of the annealed alloy #1 (Table 2).

A thermal effect at 1379 °C was observed on the heating curve of the as-cast alloy #6, which illustrated an invariant process (Fig. 3a). After annealing at 1280 °C this alloy possessed a two-phase structure (βTi, Cr) + γ (Fig. 2c). Its position was adopted on the boundary tie-line of the isothermal plane (αTi) + (βTi, Cr) + γ, with 1379 °C as its corresponding temperature. There is a great variation in the literature values of this temperature—the experimental values are higher (1433 °C[20] and 1409 °C[31]) than thermodynamic estimations (1351 °C[27] and 1361 °C[32]). According to the assumption of Witusiewicz et al.[32], the difficulty in measuring the melting temperatures of alloys from this phase region can be associated with a sharp change in the nature of phase equilibria at small decreasing

**Table 2** Solidus temperatures and phase composition of the Al-Ti-Cr alloys at subsolidus temperatures

| No | Alloy composition, at.% | | | Solidus temperature, °C (DTA data) | Heat treatment, °C (h) | Phase composition on solidus projection | Microprobe results | | | |
|----|----|----|----|----|----|----|----|----|----|----|
| | Al | Ti | Cr | | | | Phase | Composition of phase, at.% | | |
| | | | | | | | | Al | Ti | Cr |
| 1 | 45 | 50 | 5 | 1418 | 1370 (20) | (βTi, Cr) + (αTi) | (βTi, Cr) | 44.1 | 50.2 | 5.7 |
| | | | | | | | (αTi) | 46.7 | 48.9 | 4.4 |
| 2 | 50 | 2 | 48 | 1305 | 1220 (50) | (βTi, Cr) + $\gamma_3$ | (βTi, Cr) | 46.0 | 1.9 | 52.1 |
| | | | | | | | $\gamma_3$ | 58.1 | 2.3 | 39.6 |
| 3 | 50 | 10 | 40 | 1260 | 1220 (50) | (βTi, Cr) + $\gamma_3$ | (βTi, Cr) | … | … | … |
| | | | | | | | $\gamma_3$ | 55.7 | 10.0 | 34.3 |
| 4 | 50 | 25 | 25 | 1284 | 1220 (50) | τ + (βTi, Cr) | τ | 59.1 | 28.0 | 12.9 |
| | | | | | | | (βTi, Cr) | 42.0 | 23.0 | 35.0 |
| 5 | 50 | 42 | 8 | 1359[31] | 1140 (20), 1310 (20) | (βTi, Cr) + γ | (βTi, Cr) | … | … | … |
| | | | | | | | γ | 53.5 | 41.9 | 4.6 |
| 6 | 53 | 42 | 5 | 1379 | 1280 (30) | (βTi, Cr) + γ | (βTi, Cr) | … | … | … |
| | | | | | | | γ | 53.1 | 42.1 | 4.8 |
| 7 | 55 | 30 | 15 | … | 1220 (50) | τ + (βTi, Cr) | τ | 57.9 | 30.5 | 11.6 |
| | | | | | | | (βTi, Cr) | 41.4 | 29.7 | 28.9 |
| 8 | 57 | 15 | 28 | 1246[31] | 1200 (24)[58] | τ + (βTi, Cr) + $\gamma_3$ | τ | 61.8 | 23.8 | 14.4 |
| | | | | | | | (βTi, Cr) | 43.2 | 11.1 | 45.7 |
| 9 | 60 | 2 | 38 | 1272 | 1220 (50) | $\gamma_3$ | $\gamma_3$ | 54.7 | 12.2 | 33.1 |
| | | | | | | | $\gamma_3$ | … | … | … |
| 11 | 60 | 20 | 20 | 1244[31] | 1200 (24)[58] | τ + (βTi, Cr) + $\gamma_3$ | τ | 63.1 | 22.6 | 14.3 |
| | | | | | | | (βTi, Cr) | 45.6 | 11.1 | 43.3 |
| | | | | | | | $\gamma_3$ | 55.8 | 11.8 | 32.4 |
| 12 | 60 | 31 | 9 | 1376 | 1280 (30) | τ | τ | … | … | … |
| 13 | 65 | 20 | 15 | 1216 | 1200 (24)[58] | τ + $\gamma_3$ | τ | 66.8 | 21.6 | 11.6 |
| | | | | | | | $\gamma_3$ | 62.6 | 7.8 | 29.6 |
| 14 | 65 | 27 | 8 | 1362 | 1280 (30) | τ | τ | … | … | … |
| 15 | 70 | 22 | 8 | 1200 | 840 (20),990 (20),1140 (20) | τ + $\gamma_3$ + ε | τ | 67.3 | 22.3 | 10.4 |
| | | | | | | | $\gamma_3$ | 62.8 | 5.4 | 31.8 |
| | | | | | | | ε | 73.9 | 20.9 | 5.2 |
| 16 | 70 | 25 | 5 | 1355 | 1220 (50) | ε + τ | ε | … | … | … |
| | | | | | | | τ | … | … | … |
| 17 | 72 | 20 | 8 | 1202 | 1140 (20) | τ + $\gamma_3$ + ε | τ | … | … | … |
| | | | | | | | $\gamma_3$ | … | … | … |
| | | | | | | | ε | … | … | … |
| 18 | 73 | 6 | 21 | 1045 | 840 (20),990 (20) | $\gamma_3$ + ε | $\gamma_3$ | … | … | … |
| | | | | | | | ε | 75.1 | 8.4 | 16.5 |
| 19 | 75 | 10 | 15 | 1083 | 840 (20), 990 (20) | $\gamma_3$ + ε | $\gamma_3$ | … | … | … |
| | | | | | | | ε | … | … | … |
| 20 | 78 | 14 | 8 | 874 | 780 (25) | η + ε | η | 86.5 | 1.8 | 11.7 |
| | | | | | | | ε | 74.7 | 18.1 | 7.2 |
| 21 | 80 | 12 | 8 | 870 | 600 (45) | θ + ε | θ | 86.5 | 1.2 | 12.3 |
| | | | | | | | ε | 74.5 | 20.2 | 5.3 |
| 22 | 84 | 2 | 14 | 960 | 600 (45), 780 (25) | η + μ + ε | η | … | … | … |
| | | | | | | | μ | … | … | … |
| | | | | | | | ε | … | … | … |

J. Phase Equilib. Diffus. (2022) 43:427–447

433

**Table 2** continued

| No | Alloy composition, at.% | | | Solidus temperature, °C (DTA data) | Heat treatment, °C (h) | Phase composition on solidus projection | Microprobe results | | | |
|----|----|----|----|----|----|----|----|----|----|----|
| | Al | Ti | Cr | | | | Phase | Composition of phase, at.% | | |
| | | | | | | | | Al | Ti | Cr |
| 23 | 85 | 10 | 5 | 664 | 600 (45) | θ + ε + (Al) | θ | 86.4 | 1.6 | 12.0 |
| | | | | | | | ε | 74.4 | 23.2 | 2.4 |
| | | | | | | | (Al) | … | … | … |
| 24 | 87 | 2 | 11 | 852 | 600 (45) | θ + ε | θ | 86.6 | 1.7 | 11.7 |
| | | | | | | | ε | 74.8 | 21.1 | 4.1 |
| 25 | 90 | 2 | 8 | 667 | 600 (45) | θ + ε + (Al) | θ | 86.8 | 1.1 | 12.1 |
| | | | | | | | ε | 74.4 | 24.8 | 0.8 |
| | | | | | | | (Al) | 99.4 | 0.2 | 0.4 |

temperatures below the solidus which change the nature of crystallization. The value obtained here (1379 °C) is closest to the data of Chen et al.[27] and Witusiewicz et al.[32]

Among the intermediate phases of the boundary binary systems Al-Ti and Al-Cr the highest solubility of the third component is observed in the ε phase based on high-temperature modification of the compound TiAl$_3$. According to the EPMA data of the two-phase (γ$_3$ + ε) alloy #18 annealed at 990 °C, located near the three-phase region γ$_3$ + ε + μ (Table 2; Fig. 2d), the solubility of chromium in this phase is about 16.5 at.%. Bright contrast inclusions in the structure of alloy #18 correspond to the impurity, probably oxidative phase. The solubility of titanium in the γ$_3$ phase is slightly lower than of chromium—11.8 at.% Al at 1245 °C, a temperature of an isothermal plane τ + (βTi, Cr) + γ$_3$. Information on the position of this plane given in the thermodynamic description[32] differs markedly from the data of the previous publication of experimental results,[31] although the temperature values are close: 1241 °C[32] versus 1246 °C.[31] However, Witusiewicz et al.[32] did not represent any primary experimental data as arguments for their conclusions about the position of the isothermal plane τ + (βTi, Cr) + γ$_3$ so results were used from the previous publication[31] and from Kriegel et al.[58] (alloys #8 and #11, Tables 2 and 3). The results of our study of the two-phase (βTi, Cr) + γ$_3$ alloy #3 (Fig. 2e) were in good agreement with previous data: the tie-line (βTi, Cr) -γ$_3$ on the corresponding linear surface, passed through the alloy #3 based on EMPA data, and passes almost parallel to the boundary tie-line of the three-phase region τ + (βTi, Cr) + γ$_3$, and within the two-phase

region (βTi, Cr) + γ$_3$ up to the boundary binary system Al-Cr there is a very small reversal of the tie-lines (Fig. 1). The solidus temperature of the alloy #3 (1260 °C; Fig. 3b, Table 2) is slightly higher than the temperature of the isothermal plane τ + (βTi, Cr) + γ$_3$. The tie-line τ-γ$_3$ is the fold of the maximum temperatures on the solidus surface, and the corresponding value of its temperature is consistent with Ichimaru et al.[17]thermodynamic assessment of Witusiewicz

The solubility of chromium in the γ phase based on TiAl reaches about 8.5 at.% at temperature of 1297 °C of the isothermal plane γ + τ + (βTi, Cr). In the rest of the intermediate phases (ζ, μ, η and θ) the solubility of the third component does not exceed 3 at.%.

The participation of the phase τ based on the ternary compound TiCr$_{0.33}$Al$_{2.67}$ in equilibria during crystallization of alloys was confirmed and the position of its homogeneity range on the solidus surface was derived. Its maximum aluminum extent is about 12 at.%, and maximum titanium and chromium extent—about 9 at.% (Fig. 1). The obtained information is close to the previous experimental work[31] and significantly differs from the thermodynamic assessment of Witusiewicz et al.[32] Within the homogeneity range the alloys, which being annealed at subsolidus temperatures were single-phase (τ)—#12 and #14 (Table 2, Fig. 2f).

Alloys # 15 and # 17, annealed at 1140 °C have τ + γ$_3$ + ε phases (Table 2, Fig. 2g, h) gave the position of the corresponding three-phase region, which correlates with the results of the previous study of the 69Al-14Ti-17Cr (at.%) alloy annealed at 1150 °C[31] and differs from the data of thermodynamic evaluation,[32] in which,

**Table 3** Phase composition of the Al-Ti-Cr alloys and lattice parameters of the phases according to the XRD data

| No | Al | Ti | Cr | Heat treatment, °C (h) | Phase composition | Lattice parameters of the phases, nm |
|---|---|---|---|---|---|---|
| 1 | 45 | 50 | 5 | As-cast | (βTi, Cr) + (αTi) | (βTi, Cr): $a = 0.3300(5)$, (αTi): $a = 0.2960(3)$, $c = 0.4700(8)$ |
| 2 | 50 | 2 | 48 | As-cast | (βTi, Cr) + $\gamma_3$ | (βTi, Cr): $a = 0.2892(5)$, $\gamma_3$: $a = 0.9909(4)$ |
|  |  |  |  | 1220 (50) | (βTi, Cr) + $\gamma_3$ | (βTi, Cr): $a = 0.29048(8)$, $\gamma_3$: $a = 0.9095(7)$ |
| 3 | 50 | 10 | 40 | As-cast | (βTi, Cr) + $\gamma_3$ | (βTi, Cr): $a = 0.3050(9)$, $\gamma_3$: $a = 0.9137(5)$ |
|  |  |  |  | 1220 (50) | (βTi, Cr) + $\gamma_3$ | (βTi, Cr): $a = 0.3048(2)$, $\gamma_3$: $a = 0.9102(1)$ |
| 4 | 50 | 25 | 25 | As-cast | (βTi, Cr) + τ | (βTi, Cr): $a = 0.3090(1)$, τ: $a = 0.3961(9)$ |
|  |  |  |  | 1220 (50) | (βTi, Cr) + τ | (βTi, Cr): $a = 0.3088(2)$, τ: $a = 0.3960(0)$ |
| 5 | 50 | 42 | 8 | As-cast | (βTi, Cr) + (αTi) + γ | (βTi, Cr): $a = 0.3304(4)$, (αTi): $a = 0.2958(1)$, $c = 0.4673(4)$, γ: $a = 0.3998(7)$, $c = 0.4065(7)$ |
|  |  |  |  | 1140 (20), 1310 (20) | (βTi, Cr) + (αTi) + γ | (βTi, Cr): $a = 0.33074(4)$, (αTi): $a = 0.2959(8)$, $c = 0.4701(9)$, γ: $a = 0.3992(7)$, $c = 0.4040(6)$ |
| 6 | 53 | 42 | 5 | As-cast | (αTi) + γ | (αTi): $a = 0.2952(1)$, $c = 0.4632(4)$, γ: $a = 0.3999(9)$, $c = 0.4062(0)$ |
|  |  |  |  | 1280 (30) | (βTi, Cr) + (αTi) + γ | (βTi, Cr): $a = 0.3306(8)$, (αTi): $a = 0.2960(0)$, γ: $a = 0.3987(7)$, $c = 0.4067(4)$ |
| 7 | 55 | 30 | 15 | As-cast | τ + (βTi, Cr) | τ: $a = 0.3958(5)$, (βTi, Cr): $a = 0.3089(6)$ |
|  |  |  |  | 1220 (50) | τ + (βTi, Cr) | τ: $a = 0.3956(6)$, (βTi, Cr): $a$ not determined |
| 8 | 57 | 15 | 28 | 1200 (24) [31] | τ + (βTi, Cr) + $\gamma_3$ | τ: $a = 0.39486(4)$, (βTi, Cr): $a = 0.30780(0)$, $\gamma_3$: $a = 0.914241(1)$ |
| 9 | 60 | 2 | 38 | As-cast | $\gamma_3$ | $\gamma_3$: $a = 0.9086(3)$ |
|  |  |  |  | 1220 (50) | $\gamma_3$ | $\gamma_3$: $a = 0.9123(9)$ |
| 10 | 60 | 10 | 30 | As-cast | τ + $\gamma_3$ | τ: $a$ not determined, $\gamma_3$: $a = 0.9090(8)$ |
| 11 | 60 | 20 | 20 | 1200 (24) [31,58] | τ + (βTi, Cr) + $\gamma_3$ | τ: $a = 0.39471(5)$, (βTi, Cr): $a = 0.30760(1)$, $\gamma_3$: $a = 0.91454(5)$ |
| 12 | 60 | 31 | 9 | As-cast | τ | τ: $a = 0.3955(6)$ |
|  |  |  |  | 1280 (30) | τ | τ: $a = 0.3956(3)$ |
| 13 | 65 | 20 | 15 | As-cast | τ + $\gamma_3$ | τ: $a = 0.3958(3)$, $\gamma_3$: $a = 0.9107(8)$ |
| 14 | 65 | 27 | 8 | As-cast | τ | τ: $a = 0.3955(3)$ |
|  |  |  |  | 1280 (30) | τ | τ: $a = 0.3954(7)$ |
| 15 | 70 | 22 | 8 | As-cast | τ + $\gamma_3$ + ε | τ: $a = 0.3961(7)$, $\gamma_3$: $a = 0.9091(2)$, ε: $a = 0.3842(7)$, $c = 0.8621(8)$ |
|  |  |  |  | 840 (20), 990 (20), 1140 (20) | τ + $\gamma_3$ + ε | τ: $a = 0.3957(5)$, $\gamma_3$: $a$ is not determined, ε: $a = 0.3842(6)$, $c = 0.8613(2)$ |
| 16 | 70 | 25 | 5 | 1220 (50) | ε + τ | ε: $a = 0.3843(7)$, $c = 0.8607(5)$, τ: $a = 0.3958(4)$ |
| 17 | 72 | 20 | 8 | As-cast | τ + $\gamma_3$ + ε | τ: $a = 0.3958(2)$, $\gamma_3$: $a = 0.9085(7)$, ε: $a = 0.3848(6)$, $c = 0.8616(8)$ |
|  |  |  |  | 1140 (20) | τ + $\gamma_3$ + ε | τ: $a = 0.3958(5)$, $\gamma_3$: $a = 0.9106(6)$, ε: $a = 0.3845(8)$, $c = 0.8604(0)$ |
| 18 | 73 | 6 | 21 | As-cast | τ + $\gamma_3$ + ε | τ: $a$ not determined, $\gamma_3$: $a = 0.9085(7)$, ε: $a = 0.3761(5)$, $c = 0.8709(0)$ |
| 19 | 75 | 10 | 15 | As-cast | $\gamma_3$ + ε | $\gamma_3$: $a = 0.9100(1)$, ε: $a = 0.3847(4)$, $c = 0.8643(2)$ |
|  |  |  |  | 840 (20), 990 (20) | $\gamma_3$ + ε | $\gamma_3$: $a$ not determined, ε: $a = 0.3849(0)$, $c = 0.8608(8)$ |
| 20 | 78 | 14 | 8 | As-cast | η + ε | η: $a = 1.2887(0)$, $b = 0.7651(0)$, $c = 1.0638(3)$, $\beta = 122.1(9)°$; ε: $a = 0.3841(2)$, $c = 0.8600(9)$ |
|  |  |  |  | 780 (25) | η + ε | η: $a = 1.2823(6)$, $b = 0.7641(8)$, $c = 1.0591(4)$, $\beta = 122.0(1)°$; ε: $a = 0.3841(5)$, $c = 0.8605(2)$ |

**Table 3** continued

| No | Alloy composition, at.% | | | Heat treatment, °C (h) | Phase composition | Lattice parameters of the phases, nm |
|----|------|------|------|------|------|------|
|    | Al | Ti | Cr |   |   |   |
| 21 | 80 | 12 | 8 | As-cast | θ + ε | θ: $a = 2.5193(3)$, $b = 0.7563(5)$, $c = 1.09942(9)$, $β = 128.688(8)°$, ε: $a = 0.3840(7)$, $c = 0.8593(5)$ |
|    |    |    |   | 600 (45) | θ + ε | θ: $a = 2.5233(2)$, $b = 0.7574(5)$, $c = 1.09494(4)$, $β = 128.564(7)°$, ε: $a = 0.3841(8)$, $c = 0.8604(1)$ |
| 22 | 84 | 2 | 14 | As-cast | η + μ + ε | η: $a = 1.2788(0)$, $b = 0.7752(0)$, $c = 1.0625(8)$, $β = 121.6(9)°$ μ: $a = 2.0103(3)$, $c = 2.4785(7)$, ε: $a = 0.3843(3)$, $c = 0.8623(6)$ |
|    |    |    |   | 600 (45), 780 (25) | η + μ + ε | η: $a = 1.2869(7)$, $b = 0.7639(9)$, $c = 1.0645(0)$, $β = 122.1(8)°$ μ: $a = 2.0104(4)$, $c = 2.4801(0)$, ε: $a = 0.3840(0)$, $c = 0.8709(0)$ |
| 23 | 85 | 10 | 5 | 600 (45) | θ + ε + (Al) | θ: $a = 2.5185(7)$, $b = 0.7561(7)$, $c = 1.0938(0)$, $β = 128.640(0)°$, ε: $a = 0.3844(4)$, $c = 0.8613(4)$, (Al): $a = 0.4045(6)$ |
| 24 | 87 | 2 | 11 | 600 (45) | θ + ε | θ: $a = 2.5168(8)$, $b = 0.7511(2)$, $c = 1.1046(1)$, $β = 128.591(5)°$, ε: $a = 0.3854(8)$, $c = 0.8548(0)$ |
| 25 | 90 | 2 | 8 | As-cast | θ + ε + (Al) | θ: $a = 2.5188(2)$, $b = 0.7568(6)$, $c = 1.0955(6)$, $β = 128.660(7)°$, ε: $a = 0.3844(1)$, $c = 0.8635(8)$, (Al): $a = 0.4044(7)$ |
|    |    |    |   | 600 (25) | θ + ε + (Al) | θ: $a = 2.5215(0)$, $b = 0.7577(4)$, $c = 1.0957(1)$, $β = 128.721(0)°$, ε: $a = 0.3869(6)$, $c = 0.8581(8)$, (Al): $a = 0.4048(7)$ |

apparently, these results were not sufficiently taken into account. As for the temperature of the isothermal plane $τ + γ_3 + ε$, its similar values obtained here based on the DTA data of as-cast alloys (Table 2, Fig. 3c, d) #15 (1200 °C), #17 (1202 °C) and nonequilibrium crystallized alloy #16 (1200 °C), identical to those given by various authors-1200 °C[20] and 1201 °C.[31,32]

Figure 2(i) shows the microstructure of the alloy #25 annealed at 600 °C during 20 h. It confirms the existence of a three-phase region $θ + ε + (Al)$, and the coordinates of the apexes are taken according to the EPMA of this alloy (Table 2).

As a result of this study, the solidus surface of the Al-Ti-Cr system in the range of compositions 40-100 at.% Al was specified. It is formed by fourteen single-phase surfaces corresponding to a continuous series of solid solutions between βTi and chromium, solid solution based on αTi, phases based on binary compounds TiAl, $Ti_{2+x}Al_{5-x}$, $TiAl_3$ (high-temperature modification and modification, stable at room temperature), $Cr_5Al_8$ ($γ_3$, $γ_2$ and $γ_1$ phases), $CrAl_4$, $Cr_2Al_{11}$, $CrAl_7$ and the ternary compound τ. The constituent parts of the surface include 22 tie-line surfaces limiting the two-phase volumes as well as 13 isothermal planes.

### 4.2 Liquidus Surface

The components of the liquidus surface of the Al-Ti-Cr system in the range of compositions 40-100 at.% Al, in accordance with the solidus surface constitution, are the primary solidification surfaces corresponding to a continuous series of solid solutions between βTi and chromium, solid solution based on αTi, phases based on binary compounds TiAl, $Ti_{2+x}Al_{5-x}$, $TiAl_3$ (high-temperature modification and modification, stable at room temperature), $Cr_5Al_8$ ($γ_3$, $γ_2$ and $γ_1$ phases), $CrAl_4$, $Cr_2Al_{11}$, $CrAl_7$ and the ternary compound τ. Information on the sequence of reactions that occur during the crystallization of alloys, obtained from metallographic studies of as-cast samples, in combination with DTA and x-ray diffraction data, allowed the derivation, in addition to the primary crystallized phase, the position of monovariant curves as well as direction and nature of processes (congruent or incongruent) flowing along them. This also made it possible to determine the composition of invariant points and the type of reactions that take place in them, which later allowed the building of a melting diagram of the system (Part 4.3).

The liquidus surface projection constructed is shown in Fig. 4. The positions of the isotherms plotted on the projection by solid lines were determined from the values of the liquidus temperatures of the alloys in the ternary system (Table 4, Fig. 3), taking into account the corresponding temperatures in the boundary binary systems.

436

J. Phase Equilib. Diffus. (2022) 43:427–447
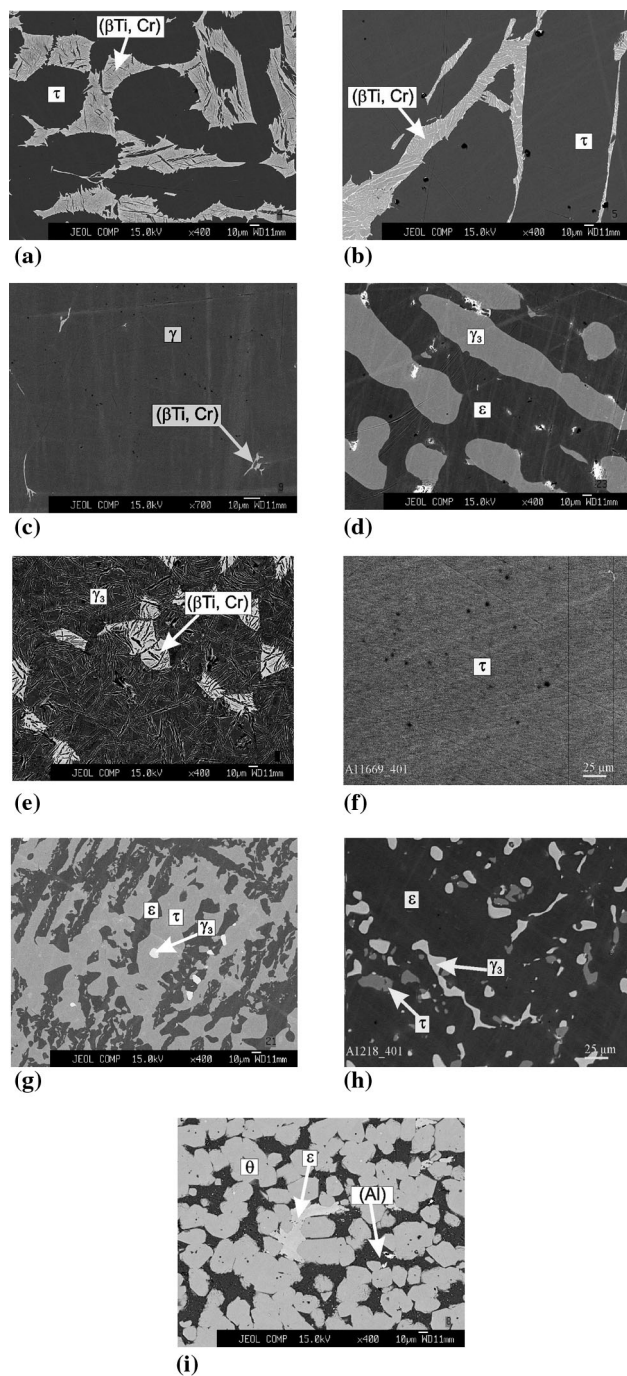


**Fig. 2** Microstructure of annealed alloys of the Al-Ti-Cr system in the range of compositions 40-100 at.% Al: (a) 50Al-25Ti-25Cr (#4) 1220 °C 50 h, × 400, τ + (βTi, Cr); (b) 55Al-30Ti-15Cr (#7) 1220 °C 50 h, × 400, τ + (βTi, Cr); (c) 53Al-42Ti-5Cr (#6) 1280 °C 30 h, × 700, (βTi, Cr) + γ; (d) 73Al-6Ti-21Cr (#18) 840 °C 20 h, 990 °C 20 h, × 400, $γ_3$ + ε; (e) 50Al-10Ti-40Cr (#3), × 400, (βTi, Cr) + $γ_3$; (f) 60Al-31Ti-9Cr (#10), 1280 °C 30 h, × 400, τ; (g) 70Al-22Ti-8Cr (#15) 840 °C 20 h, 990 °C 20 h, 1140 °C 20 h, × 400, τ + $γ_3$ + ε; (h) 72Al-20Ti-8Cr (#17) 1140 °C 20 h, × 400, τ + $γ_3$ + ε; (i) 90Al-2Ti-8Cr (#25) 600 °C 20 h, × 400, θ + ε + (Al)
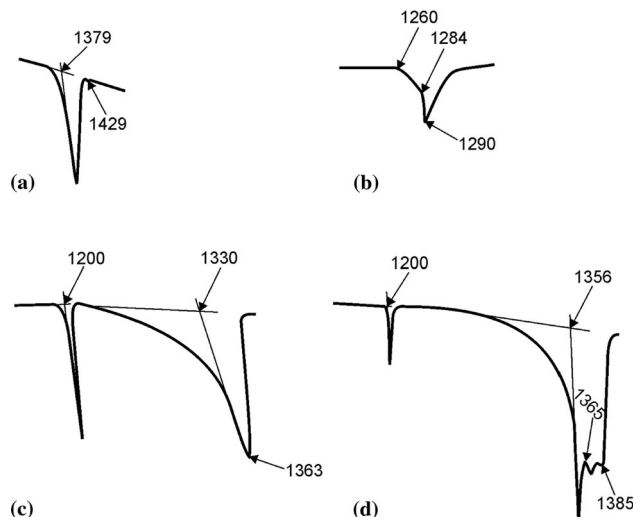


**Fig. 3** Fragments of heating curves for alloys of the Al-Ti-Cr system in the range of compositions 40-100 at.% Al: a 53Al-42Ti-5Cr (#6); b 50Al-10Ti-40Cr (#3); c 70Al-22Ti-8Cr (#15); d 70Al-25Ti-5Cr (#16)

The primary solidification surface of (βTi, Cr) Ti$p_1U_2$-$U_4E_1p_6$CrTi extends deep into the ternary system to 60 at.% Al corresponding to the point $p_6$ in the boundary binary system Al-Cr. Its position was determined from metallography and EMPA data of as-cast alloys #1, #2, #3 and #4 in which a continuous series of solid solutions between βTi and chromium crystallize primarily (Table 4, Fig. 5a, b) taking into account the corresponding data of as-cast alloys #5 and #9 in which a primary constituents are already αTi-based solid solution and the $γ_3$ phase respectively (Table 4, Fig. 5c). Location of the primary solidification surface of (βTi, Cr) was specified comparing both the previous experimental work[31] and from the thermodynamic assessment of Witusiewicz et al.[32] The temperature difference on the primary solidification surface of (βTi, Cr) is from 1863 °C (pure chromium congruent melting temperature) to 1246 °C, the temperature of invariant four-phase equilibrium with the participation of the liquid $L_{E1}$ ↔ τ + (βTi, Cr) + $γ_3$. This surface is separated from the primary solidification surfaces of (αTi), γ, τ and $γ_3$ phases by the boundary curves $p_1U_2$, $U_2U_4$, $U_4E_1$ and $E_1p_6$, respectively (Fig. 4). The first of these curves originates at point $p_1$ of the binary system Al-Ti at a temperature of 1491 °C, which corresponds to the incongruent process l + (βTi) ↔ (αTi). It passes between the alloys #1 and #5, in which different phases-(βTi, Cr) and (αTi) are primarily crystallized, respectively (Table 4). Position of the monovariant curve $U_4E_1$ was established taking into account microstructure and microprobe analysis data of the as-cast alloys #4 and #7 containing the primary constituents (βTi, Cr) and τ phases respectively (Table 4, Fig. 5b, d).

The primary solidification surface of (αTi) $p_1p_2U_2p_1$ extends from the boundary binary system Al-Ti inside the ternary one up to 12 at.% Cr (Fig. 4). Its decrease occurs from the temperature of 1491 °C at point $p_1$ both in the directions of the point $p_2$ (at 1456 °C) and deep into the ternary system to a temperature of 1379 °C at point $U_2$.

The primary solidification surface of the γ phase $p_2U_2$-$U_4p_4U_1p_3p_2$ is elongated in the direction of chromium, it reaches 17 at.% of this component. The primary solidification surface decreases from the temperatures of 1456 °C and 1432 °C at points $p_2$ and $p_3$ respectively in the boundary system Al-Ti to a temperature of 1297 °C at point $U_4$.

The primary solidification surface of the τ phase $U_1$-$U_3U_5e_1E_1U_4p_4U_1$ is located in a wide concentration range within the ternary system. Its extent by aluminum content is more than 23 at.%, by titanium content—more than 25 at.%, by chromium content—more than 19 at.%. Its position was determined from metallography and EMPA data of as-cast alloys #7, #11, #13, #14, #15 and #17 in which the τ phase crystallizes primarily (Table 4, Fig. 5d, e). The highest temperature on the surface corresponds to the maximum invariant point $p_{4(max)}$ corresponding to the invariant reaction L + γ ↔ τ (1412 °C), the lowest, 1201 °C, is the temperature of invariant four-phase equilibrium with the participation of the liquid $L_{U5} + τ ↔ γ_3 + ε$.



**Fig. 4** Liquidus surface projection of the Al-Ti-Cr system in the range of compositions 40-100 at.% Al: open circle—alloy composition

Curve $E_1U_5$ is the boundary for the primary solidification surfaces of the τ and $γ_3$ phases. It passes to the left of the alloys #10 and #18, in which the $γ_3$ phase crystallizes primarily (Table 4, Fig. 5f, g). The primary solidification surface of the $γ_3$ phase is significantly elongated in the direction of aluminum, it reaches 28 at.% Al. The exact position of the primary solidification surfaces of the $γ_1$ and $γ_2$ phases has not been established, their extent is extremely small.

Since the Al-Ti boundary binary system is accepted according to the thermodynamic description obtained by Witusiewicz et al.[33] then peculiarities of crystallization of the TiAl₃ phase modifications are consistent with the data of this article and correspond to those presented in a thermodynamic description.[32]

In accordance with constitution of the solidus surface of the Al-Ti-Cr system and the character of the equilibria involving modifications of the TiAl₃-based phase in the boundary binary system Al-Ti, a high-temperature modification ε takes part in four-phase invariant equilibria with participation of liquid at 1355, 1201, 1035, 960 and 874 °C (Table 5) while the modification TiAl₃ (r) that is stable at room temperature takes part in equilibria at 856 °C and 666 °C. The primary solidification surface of the TiAl₃-based phase $p_5U_3U_5U_8P_1U_9P_2P_3p_{10}p_5$ the surface decreases counterclockwise from a temperature of 1396 °C at point $p_5$ in the boundary system Al-Ti deep into the ternary system and back into the system Al-Ti to a temperature of 665.6 °C at point $p_{10}$. Its extent by chromium content is about 19 at.% corresponding a point $U_5$. Its position was determined from metallography and EMPA data of as-cast alloys #19, #20, #21, #23 and #25 in which the TiAl₃-based phase crystallize primarily (Table 4, Fig. 5h, i).

The primary solidification surfaces of the μ, θ and η phases extended along side Al-Cr of the concentration triangle. Maximum solubility of titanium in the μ phase is equal to 3.0 at.% while in the θ and η phases—0.8 and 0.3 at.% respectively. In the as-cast alloy #22 the μ phase crystallizes primarily and then—eutectic (ε + μ) and the η phase (Table 4). The primary solidification surface of (Al) is very small in extent.

As a result of our study, it was established that the highest temperature on the liquidus surface of the Al-Ti-Cr system in the range of compositions 40-100 at.% Al corresponds to the melting point of pure chromium (1863 °C), the lowest—to the melting point of pure aluminum (660.452 °C).
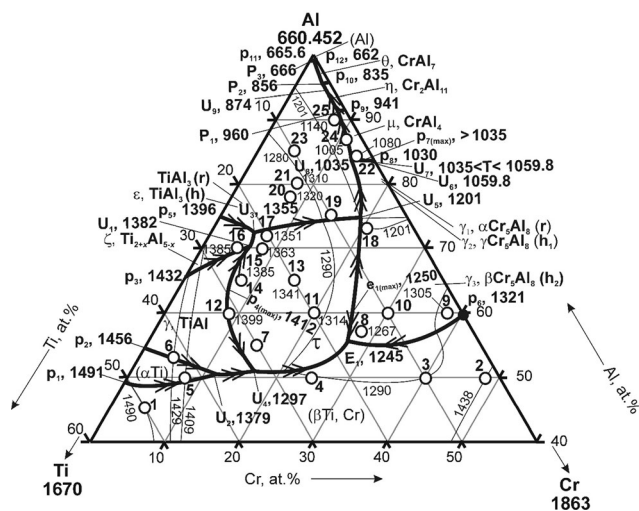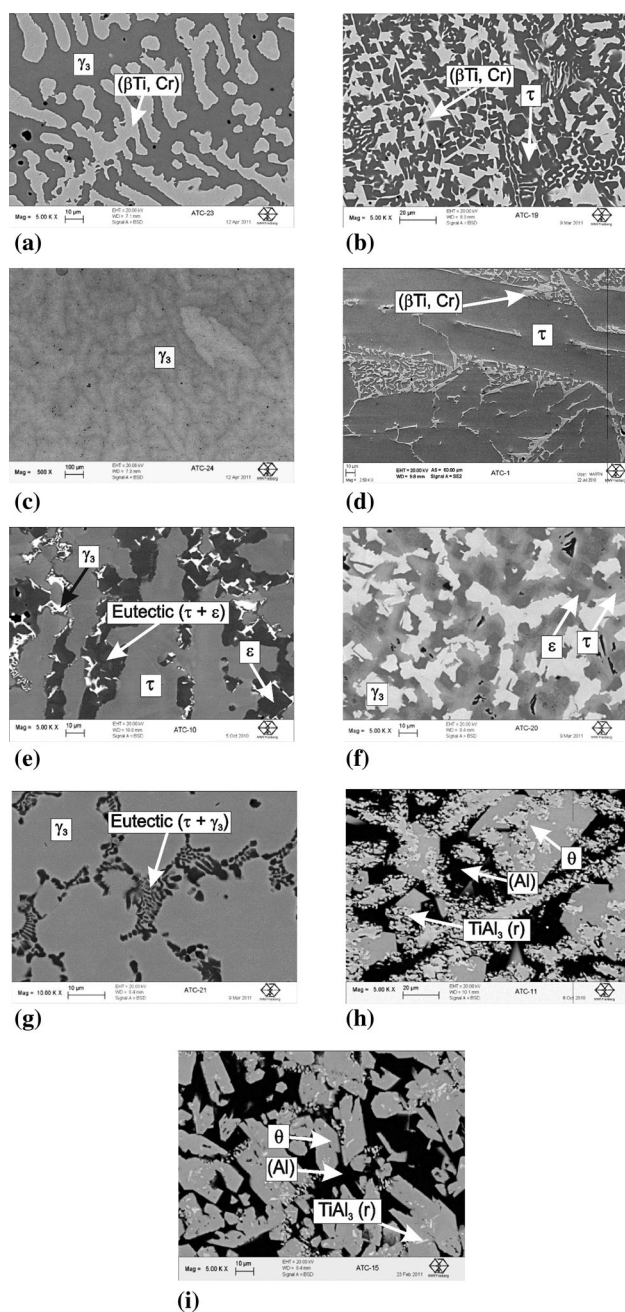
**Table 4** Liquidus temperatures and phase composition of the Al-Ti-Cr as-cast alloys

| No | Alloy composition, at.% | | | Liquidus temperature, °C (DTA data) | Phase composition in as-cast state | Phase | Composition of phase, at.% | | |
|---|---|---|---|---|---|---|---|---|---|
| | Al | Ti | Cr | | | | Al | Ti | Cr |
| 1 | 45 | 50 | 5 | 1490 | (βTi, Cr)* + (αTi) | (βTi, Cr) | 44.2 | 49.2 | 6.6 |
| | | | | | | (αTi) | 48.8 | 48.1 | 3.1 |
| 2 | 50 | 2 | 48 | 1438 | (βTi, Cr)* + γ3 | (βTi, Cr) | 43.2 | 1.6 | 55.2 |
| | | | | | | γ3 | 58.4 | 2.4 | 39.2 |
| 3 | 50 | 10 | 40 | 1290 | (βTi, Cr)* + eutectic | (βTi, Cr) | 45.4 | 9.7 | 44.7 |
| | | | | | | Eutectic ((βTi, Cr) + γ3) | 55.4 | 10.3 | 34.3 |
| 4 | 50 | 25 | 25 | 1290 | (βTi, Cr)* + τ | (βTi, Cr) | 40.2 | 22.4 | 37.4 |
| | | | | | | τ | 60.5 | 26.5 | 13.0 |
| 5 | 50 | 42 | 8 | 1409 [31] | (αTi)* + (βTi, Cr) + γ | (αTi) | ... | ... | ... |
| | | | | | | (βTi, Cr) | ... | ... | ... |
| | | | | | | γ | ... | ... | ... |
| 6 | 53 | 42 | 5 | 1429 | (αTi)* + γ | (αTi) | ... | ... | ... |
| | | | | | | γ | ... | ... | ... |
| 7 | 55 | 30 | 15 | ... | τ* + (βTi, Cr) | τ | 58.9 | 31.1 | 10.0 |
| | | | | | | (βTi, Cr) | 30.2 | 28.2 | 41.6 |
| 8 | 57 | 15 | 28 | 1267 [31] | γ3* + eutectic (τ + γ3) + eutectic (τ + (βTi, Cr) + γ3) | γ3 | ... | ... | ... |
| | | | | | | (τ + γ3) Eutectic | ... | ... | ... |
| | | | | | | Eutectic (τ + (βTi, Cr) + γ3) | ... | ... | ... |
| 9 | 60 | 2 | 38 | 1305 | γ3 | γ3 | ... | ... | ... |
| 10 | 60 | 10 | 30 | ... | *γ3* + eutectic (τ + γ3) | γ3 | ... | ... | ... |
| 11 | 60 | 20 | 20 | 1314 [31] | τ* + eutectic (τ + γ3) + eutectic (τ + (βTi, Cr) + γ3) | τ | ... | ... | ... |
| | | | | | | Eutectic (τ + γ3) | ... | ... | ... |
| | | | | | | Eutectic (τ + (βTi, Cr) + γ3) | ... | ... | ... |
| 12 | 60 | 31 | 9 | 1399 | τ* | τ | ... | ... | ... |
| 13 | 65 | 20 | 15 | 1341 | τ* + eutectic (τ + γ3) | τ | ... | ... | ... |
| | | | | | | Eutectic (τ + γ3) | ... | ... | ... |
| 14 | 65 | 27 | 8 | 1385 | τ* | τ | ... | ... | ... |
| 15 | 70 | 22 | 8 | 1363 | τ* + eutectic (τ + ε) + ε + γ3 | τ | 68.9 | 24.1 | 7.0 |
| | | | | | | Eutectic (τ + ε) | 73.0 | 20.1 | 6.9 |
| | | | | | | ε | 76.2 | 20.9 | 2.9 |

**Table 4** continued

| No | Alloy composition, at.% | | | Liquidus temperature, °C (DTA data) | Phase composition in as-cast state | Phase | Microprobe results Composition of phase, at.% | | |
|----|----|----|----|----|----|----|----|----|----|
| | Al | Ti | Cr | | | | Al | Ti | Cr |
| 16 | 70 | 25 | 5 | 1385 | ζ* + τ + ε | ζ | ... | ... | ... |
| | | | | | | τ | ... | ... | ... |
| | | | | | | ε | ... | ... | ... |
| 17 | 72 | 20 | 8 | 1351 | τ* + eutectic (τ + ε) + ε + γ₃ | τ | ... | ... | ... |
| | | | | | | Eutectic (τ + ε) | ... | ... | ... |
| | | | | | | ε | ... | ... | ... |
| | | | | | | γ₃ | ... | ... | ... |
| 18 | 73 | 6 | 21 | 1201 | γ₃* + τ + ε | γ₃ | 69.0 | 2.1 | 28.9 |
| | | | | | | τ | ... | ... | ... |
| | | | | | | ε | 75.2 | 8.1 | 16.7 |
| 19 | 75 | 10 | 15 | ... | ε* + eutectic | ε | 75.3 | 17.1 | 7.6 |
| | | | | | | Eutectic (ε + γ₃) | 75.8 | 6.0 | 18.2 |
| 20 | 78 | 14 | 8 | 1320 | **ε* + η** | ε | 75.2 | 19.0 | 5.8 |
| | | | | | | η | 86.2 | 1.1 | 12.7 |
| 21 | 80 | 12 | 8 | 1310 | **ε* + θ** | ε | 76.0 | 21.1 | 2.9 |
| | | | | | | θ | 87.4 | 1.2 | 11.4 |
| 22 | 84 | 2 | 14 | 1080 | μ* + eutectic (ε + μ) + η | μ | 81.1 | 0.4 | 18.5 |
| | | | | | | Eutectic (ε + μ) | 85.0 | 2.1 | 12.7 |
| | | | | | | η | 87.3 | 0.5 | 12.2 |
| 23 | 85 | 10 | 5 | 1280 | TiAl₃ (r)* + θ + (Al) | TiAl₃ (r) | 75.7 | 22.4 | 1.9 |
| | | | | | | θ | 88.1 | 1.1 | 10.8 |
| | | | | | | (Al) | 99.4 | 0.4 | 0.2 |
| 24 | 87 | 2 | 11 | 1005 | ... | ... | ... | ... | ... |
| 25 | 90 | 2 | 8 | 1140 | TiAl₃ (r)* + θ + (Al) | TiAl₃ (r) | 75.5 | 21.2 | 3.3 |
| | | | | | | θ | 87.6 | 0.8 | 11.6 |
| | | | | | | (Al) | 99.2 | 0.4 | 0.4 |

* the primary phase

440

J. Phase Equilib. Diffus. (2022) 43:427–447



**Fig. 5** Microstructure of as-cast alloys of the Al-Ti-Cr system in the range of compositions 40-100 at.% Al: a 50Al-2Ti-48Cr (#2), × 1000, (βTi, Cr)* + γ₃; b 50Al-25Ti-25Cr (#4), × 1000, (βTi, Cr)* + τ; c 60Al-2Ti-38Cr (#8), × 100, γ₃*; d 55Al-30Ti-15Cr (#7), × 500, τ* + (βTi, Cr); e 70Al-22Ti-8Cr (#15), × 1000, τ* + eutectic (τ + ε) + ε + γ₃; f 73Al-6Ti-21Cr (#18), × 400, γ₃* + τ + ε; g 60Al-10Ti-30Cr (#10), × 1500, γ₃* + eutectic (τ + γ₃); h 85Al-10Ti-5Cr (#23), × 400, TiAl₃ (r)* + θ + (Al); i 90Al-2Ti-8Cr (#25), × 400, TiAl₃ (r)* (the lightest small grains) + θ + (Al). An asterisk means the primary phase

### 4.3 Melting Diagram and Reaction Scheme

The superposition of the liquidus and solidus surfaces of the Al-Ti-Cr system in the range of compositions 40-100 at.% Al in the form of a melting diagram is shown in Fig. 6. The existence on the solidus surface of isothermal tie-line triangles necessarily causes the formation in the system of invariant four-phase equilibria with the participation of the liquid phase, the components of which are the corresponding triangles. The congruent nature of these equilibria was established based on the presence of ternary eutectics in as-cast alloys, the coordinates of which were determined using EMPA, SEM and DTA. The coordinates of the invariant points corresponding to the incongruent processes were determined at the intersection of the corresponding monovariant curves, taking into account their location relative to the boundary tie-lines of the tie-line triangles formed by solid phases. The determining factor was the solidus and liquidus temperatures of the alloys, which indicated the sequence of processes, i.e. the direction of the reactions that took place during the crystallization of the alloys.

It has been established that thirteen invariant four-phase reactions (nine liquid transition, three peritectic and one eutectic) and three invariant three-phase reactions (two peritectic and one eutectic maxima on monovariant curves) involving liquid take place in the system. All invariant equilibria are summarized in Table 5. Figure 7 shows the Scheil diagram for solidification of Al-Ti-Cr alloys in the range of compositions 40-100 at.% Al. Compared with the results of the previous experimental studies[31] and the data of thermodynamic description of Witusiewicz et al.,[32] the compositions of equilibrium phases and temperatures for invariant equilibria L + (αTi) ↔ (βTi, Cr) + γ, L + γ τ + (βTi, Cr) and L ↔ τ + (βTi, Cr) + γ₃ are significantly clarified. The congruent nature of the equilibrium involving phases τ and γ₃ was confirmed, in contrast to the authors of,[32] who reported the reaction L + τ ↔ γ₃ (the incongruent nature of it follows from the abnormally high solubility of titanium in the γ₃ phase reported by Witusiewicz et al.,[32] while experimental evidence for this assertion has not been provided), and the value of its temperature 1250 °C, given earlier in,[31] in contrast from 1269 °C.[32] The temperature of 1035 °C of the invariant equilibrium L + γ₃ ↔ ε + μ is identical to the data[31] and,[32] but its nature, in contrast to Witusiewicz et al.[32], is transition L + γ₃ ↔ ε + μ. It was concluded that the invariant three-phase reaction corresponding to maximum on monovariant curve) L + γ₃ ↔ μ takes place in the system at a temperature higher than 1035 °C.

J. Phase Equilib. Diffus. (2022) 43:427–447

441

**Table 5** Invariant Equilibria in the Al-Ti-Cr system involving the liquid phase

| Reaction | T, °C | Type | Phase | Composition of phase, at.% | | |
|---|---|---|---|---|---|---|
| | | | | Al | Ti | Cr |
| L + γ ↔ τ | 1412 ([32], this work) | p4 (max) | L | 63.3 | 29.2 | 7.5 |
| | | | γ | 61.7 | 33.3 | 5.0 |
| | | | τ | 62.8 | 30.5 | 6.7 |
| L + γ ↔ ζ + τ | 1382 ([32], this work) | U1 | L | 70.4 | 22.9 | 6.7 |
| | | | γ | 64.0 | 32.6 | 3.4 |
| | | | ζ | 66.5 | 30.7 | 2.8 |
| | | | τ | 65.7 | 29.0 | 5.3 |
| L + (αTi) ↔ (βTi, Cr) + γ | 1379 (this work); (1433 [20], 1351 [27], 1409 [31], 1361 [32]) | U2 | L | 50.6 | 37.4 | 12.0 |
| | | | (αTi) | 47.7 | 44.4 | 5.9 |
| | | | (βTi, Cr) | 45.6 | 45.7 | 8.7 |
| | | | γ | 53.0 | 42.2 | 4.8 |
| L + ζ ↔ ε + τ | 1355 ([31], this work); (1330 [26], 1345 [27], 1367 [32]) | U3 | L | 72.3 | 21.7 | 6.0 |
| | | | ζ | 70.5 | 27.9 | 1.6 |
| | | | ε | 74.3 | 23.8 | 1.9 |
| | | | τ | 69.0 | 25.5 | 5.5 |
| L + γ ↔ τ + (βTi, Cr) | 1297 ([31], this work); (1310 [20], 1325 [27], 1299 [32]) | U4 | L | 51.0 | 32.0 | 17.0 |
| | | | γ | 55.4 | 36.3 | 8.3 |
| | | | τ | 56.9 | 32.0 | 11.2 |
| | | | (βTi, Cr) | 41.1 | 34.1 | 24.8 |
| L ↔ τ + γ3 | 1250 ([31], this work); (1269 [32]) | e1 (max) | L | 60.0 | 14.8 | 25.2 |
| | | | τ | 64.6 | 22.1 | 13.3 |
| | | | γ3 | 57.2 | 11.0 | 31.8 |
| L ↔ τ + (βTi, Cr) + γ3 | 1245 (this work); (1260 [20], 1251 [27], 1246 [31], 1241 [32]) | E1 | L | 55.5 | 17.8 | 26.7 |
| | | | τ | 62.5 | 23.2 | 14.3 |
| | | | (βTi, Cr) | 44.4 | 11.1 | 44.5 |
| | | | γ3 | 55.3 | 12.0 | 32.7 |
| L + τ ↔ γ3 + ε | 1201 ([31], this work); (1200 [20], 1201 [32]) | U5 | L | 74.8 | 6.2 | 19.0 |
| | | | τ | 67.3 | 22.4 | 10.3 |
| | | | γ3 | 63.0 | 6.1 | 30.9 |
| | | | ε | 73.9 | 20.9 | 5.2 |
| L + γ3 ↔ μ | > 1035 (this work) | p7 (max) | L | ~ 83.6 | ~ 1.5 | ~ 14.9 |
| | | | γ3 | ~ 69.0 | ~ 1.0 | ~ 30.0 |
| | | | μ | ~ 79.5 | ~ 0.8 | ~ 19.7 |
| γ2 + γ3 ↔ L + γ1 | 1059.8 ([32], this work) | U6 | γ2 | 68.0 | 0 | 32.0 |
| | | | γ3 | 68.1 | 0 | 31.9 |
| | | | L | 82.6 | 0 | 17.4 |
| | | | γ1 | 67.4 | 0 | 32.6 |
| L + γ3 ↔ γ1 + μ | 1035 < T < 1059.8 (this work); 1033 ([32]) | U7 | L | 83.7 | 0.2 | 16.1 |
| | | | γ3 | 68.8 | 0.5 | 30.7 |
| | | | γ1 | 67.9 | 0.2 | 31.9 |
| | | | μ | 80.0 | 0.5 | 19.5 |
| L + γ3 ↔ ε + μ | 1035 ([31], this work); (1034 [20]; 1035, P-type [32]) | U8 | L | 83.5 | 3.0 | 13.5 |
| | | | γ3 | 69.1 | 1.6 | 29.3 |
| | | | ε | 75.0 | 8.0 | 17.0 |
| | | | μ | 79.0 | 1.2 | 19.8 |

442

J. Phase Equilib. Diffus. (2022) 43:427–447

**Table 5** continued

| Reaction | T, °C | Type | Phase | Composition of phase, at.% | | |
|---|---|---|---|---|---|---|
| | | | | Al | Ti | Cr |
| L + ε + μ ↔ η | 960 (this work); (976 [32]) | P₁ | L | 91.6 | 0.8 | 7.6 |
| | | | ε | 75.0 | 12.6 | 12.4 |
| | | | μ | 80.3 | 1.2 | 18.5 |
| | | | η | 86.0 | 1.3 | 12.7 |
| ε + η ↔ L + TiAl₃ (r) | 874 (this work); (880 [32]) | U₉ | ε | 75.0 | 18.3 | 6.7 |
| | | | η | 86.0 | 1.7 | 12.3 |
| | | | L | 95.1 | 0.4 | 4.5 |
| | | | TiAl₃ (r) | 75.2 | 18.3 | 6.5 |
| L + TiAl₃ (r) + η ↔ θ | 856 (this work); (838 [20,31], 858 [34]) | P₂ | L | 95.9 | 0.3 | 3.8 |
| | | | TiAl₃ (r) | 75.1 | 19.8 | 5.1 |
| | | | θ | 86.5 | 1.8 | 11.7 |
| | | | η | 86.0 | 1.8 | 12.2 |
| L + TiAl₃ (r) + θ ↔ (Al) | 666 ([20,31], this work); (666.5 [32]) | P₃ | L | 99.8 | ∼ 0 | 0.2 |
| | | | TiAl₃ (r) | 76.2 | 23.0 | 0.8 |
| | | | θ | 86.6 | 1.7 | 11.7 |
| | | | (Al) | 98.9 | 0.8 | 0.3 |
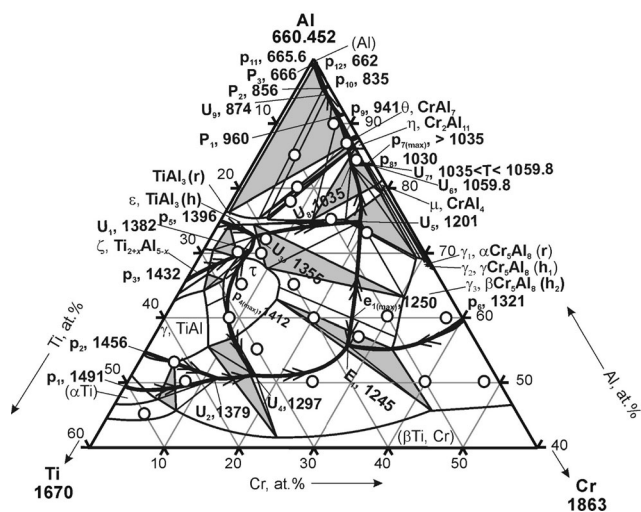


**Fig. 6** Melting diagram of the Al-Ti-Cr system in the range of compositions 40-100 at.% Al: open circle—alloy composition
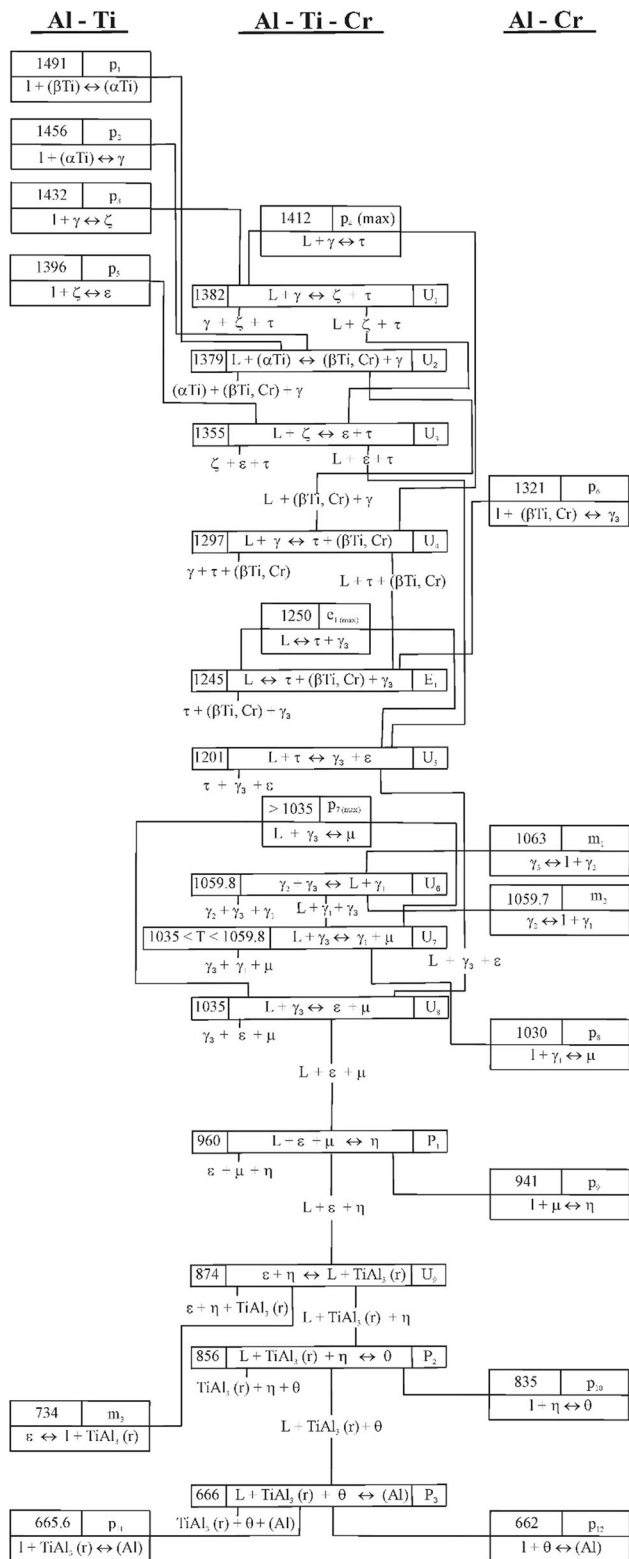
### 4.4 Isopleths

For the first time three isopleths were constructed: at 50, 60 and 70 at.% Al which demonstrate the influence of aluminum on the character of phase equilibria. The results of the study of as-cast and annealed at subsolidus temperatures alloys were used. However, preference was given to the DTA results, which established the temperatures of phase transitions in solid–liquid regions, as well as solidus and liquidus temperatures. Among the DTA curves, heating curves were preferred over cooling curves. This is due to the great supercooling of ingots during their crystallization on the hearth of the arc furnace during melting, and temperatures of the processes occurring during the crystallization of alloys can be understated.

The isopleth at 50 at.% Al (Fig. 8) intersects the primary solidification volumes of a solid solution based on αTi and a continuous series of solid solutions between βTi and chromium. The incongruent character of α-titanium crystallization, inherent in the binary system Al-Ti is still preserved in this section (L + (βTi) ↔ (αTi)). With a chromium content of about 12 at.% and aluminum about 50.5 at.%, i.e. outside the isopleth at 50 at.% Al plane it changes to congruent. On the liquidus curve of (βTi, Cr) a minimum at about 1270 °C with a chromium content of about 35 at.% occurs. From the Al-Cr boundary binary system, the phase regions at temperatures below 1200 °C are represented schematically. The temperatures of isothermal planes corresponding to four-phase invariant

## Al - Ti  Al - Ti - Cr  Al - Cr

**Al - Ti**

| 1491 | p₁ |
| 1 + (βTi) ↔ (αTi) |

| 1456 | p₂ |
| 1 + (αTi) ↔ γ |

| 1432 | p₃ |
| 1 + γ ↔ ζ |

| 1396 | p₅ |
| 1 + ζ ↔ ε |

**Al - Ti - Cr**

| 1412 | p₄ (max) |
| L + γ ↔ τ |

| 1382 | L + γ ↔ ζ + τ | U₁ |
| γ + ζ + τ | | L + ζ + τ |

| 1379 | L + (αTi) ↔ (βTi, Cr) + γ | U₂ |
| (αTi) + (βTi, Cr) - γ |

| 1355 | L + ζ ↔ ε + τ | U₃ |
| ζ + ε + τ | | L + ε + τ |

L + (βTi, Cr) + γ

| 1297 | L + γ ↔ τ + (βTi, Cr) | U₄ |
| γ + τ + (βTi, Cr) | | L + τ + (βTi, Cr) |

| 1250 | e₁(max) |
| L ↔ τ + γ₃ |

| 1245 | L ↔ τ + (βTi, Cr) + γ₃ | E₁ |
| τ + (βTi, Cr) - γ₃ |

| 1201 | L + τ ↔ γ₃ + ε | U₅ |
| τ + γ₃ + ε |

| >1035 | p₇(max) |
| L + γ₃ ↔ μ |

| 1059.8 | γ₂ - γ₃ ↔ L + γ₁ | U₆ |
| γ₂ + γ₃ + γ₁ | L + γ₁ + γ₃ |

| 1035 < T < 1059.8 | L + γ₃ ↔ γ₁ + μ | U₇ |
| γ₃ + γ₁ + μ | | L + γ₃ + ε |

| 1035 | L + γ₃ ↔ ε + μ | U₈ |
| γ₃ + ε + μ |

L + ε + μ

| 960 | L - ε - μ ↔ η | P₁ |
| ε - μ + η |

L + ε + η

| 874 | ε + η ↔ L + TiAl₃ (r) | U₉ |
| ε + η + TiAl₃ (r) | | L + TiAl₃ (r) + η |

| 856 | L + TiAl₃ (r) + η ↔ θ | P₂ |
| TiAl₃ (r) + η + θ |

L + TiAl₃ (r) + θ

| 666 | L + TiAl₃ (r) + θ ↔ (Al) | P₃ |
| TiAl₃ (r) + θ + (Al) |

**Al - Cr**

| 1321 | p₆ |
| 1 + (βTi, Cr) ↔ γ₃ |

| 1063 | m₁ |
| γ₃ ↔ 1 + γ₂ |

| 1059.7 | m₂ |
| γ₂ ↔ 1 + γ₁ |

| 1030 | p₈ |
| 1 + γ₁ ↔ μ |

| 941 | p₉ |
| 1 + μ ↔ η |

| 835 | p₁₀ |
| 1 - η ↔ θ |

| 662 | p₁₂ |
| 1 + θ ↔ (Al) |

| 734 | m₃ |
| ε ↔ 1 + TiAl₃ (r) |

| 665.6 | p₁ |
| 1 + TiAl₃ (r) ↔ (Al) |

**Fig. 7** Scheil diagram for solidification of Al-Ti-Cr alloys in the range of compositions 40-100 at.% Al

equilibria with the participation of the liquid phase, represented in the isopleth by horizontal straight lines, gradually decrease in the direction of increasing the chromium content in alloys from 1379 to 1245 °C.

With increasing aluminum content, the character of crystallization of the

Al-Ti-Cr system alloys changes markedly. In contrast to isopleth at 50 at.% Al, isopleth at 60 at.% Al (Fig. 9) intersects the primary solidification volumes of the phases γ, γ₃ and the ternary phase τ. It clearly illustrates the incongruent character of the τ phase formation from the γ phase and its joint crystallization with the γ₃ phase according to the reactions L + γ ↔ τ and L ↔ τ + γ₃, respectively. As the chromium content increases, the solidus curve of the two-phase region τ + γ₃ falls gradually. The isopleth intersects the isothermal plane, which corresponds to a four-phase invariant equilibrium involving (βTi, Cr) and phases τ and γ₃.

The isopleth at 70 at.% Al (Fig. 10) intersects the primary solidification volumes of the phases ζ, γ₃ and the ternary phase τ. Like in the case of the γ phase, the τ phase is formed from the ζ phase by peritectic reaction L + ζ ↔ τ, and the congruent character of the reaction involving the liquid and phases τ and γ₃ is preserved. With increasing the chromium content the solidus curves of the two-phase regions ε + τ and γ₃ + ε go down quite sharp. The temperatures of the isothermal planes decrease with increasing the chromium content in alloys from 1355 to 1035 °C.

Thus, the constructed isopleths of the Al-Ti-Cr system confirmed the reliability of the interpretation of the obtained results regarding constitution of liquidus, solidus and melting diagram of the system. The character of crystallization of phases on the basis of binary compounds and the ternary phase τ is drawn.

## 5 Conclusions

Phase equilibria in the Al-Ti-Cr system in the range of compositions 40-100 at.% Al have been studied using optical microscopy, scanning electron microscopy, DTA, x-ray diffraction and electron probe microanalysis. Specified solidus and liquidus surfaces, a melting diagram as their superposition, the Scheil diagram for solidification as well as series of isopleths (at 50, 60 and 70 at.% Al) were constructed for this system.

There are 13 four-phase and 3 three-phase invariant equilibria with participation of the liquid phase in the system, which are at temperatures from 1412 to 666 °C.
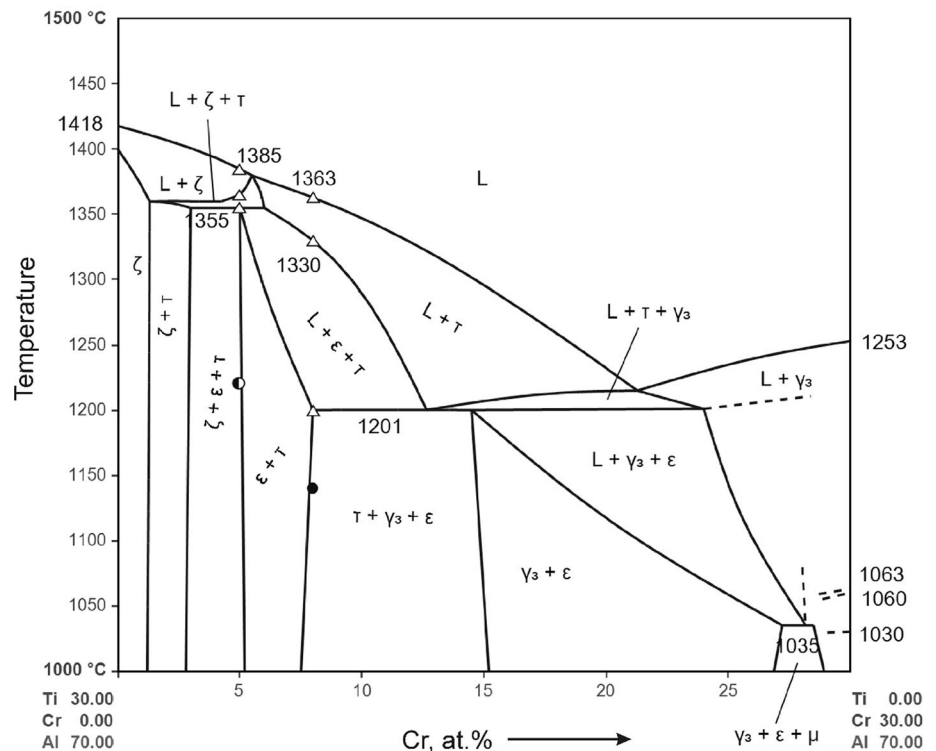
**Fig. 8** Isopleth at 50 at.% Al: half vertical filled circle—two-phase sample; open triangle—DTA data
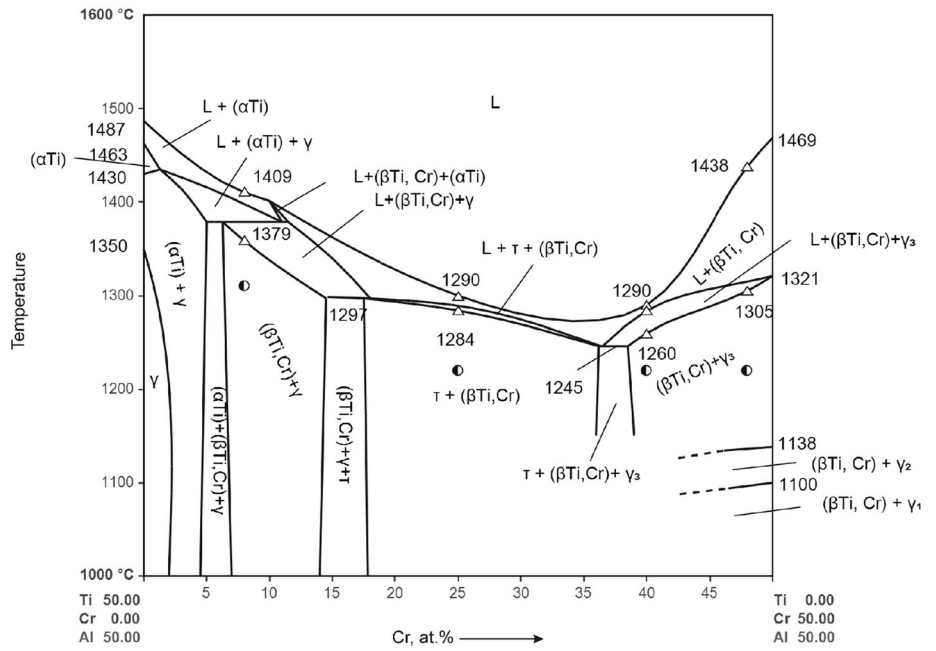


**Fig. 9** Isopleth at 60 at.% Al: open circle—single-phase sample; open triangle —DTA data
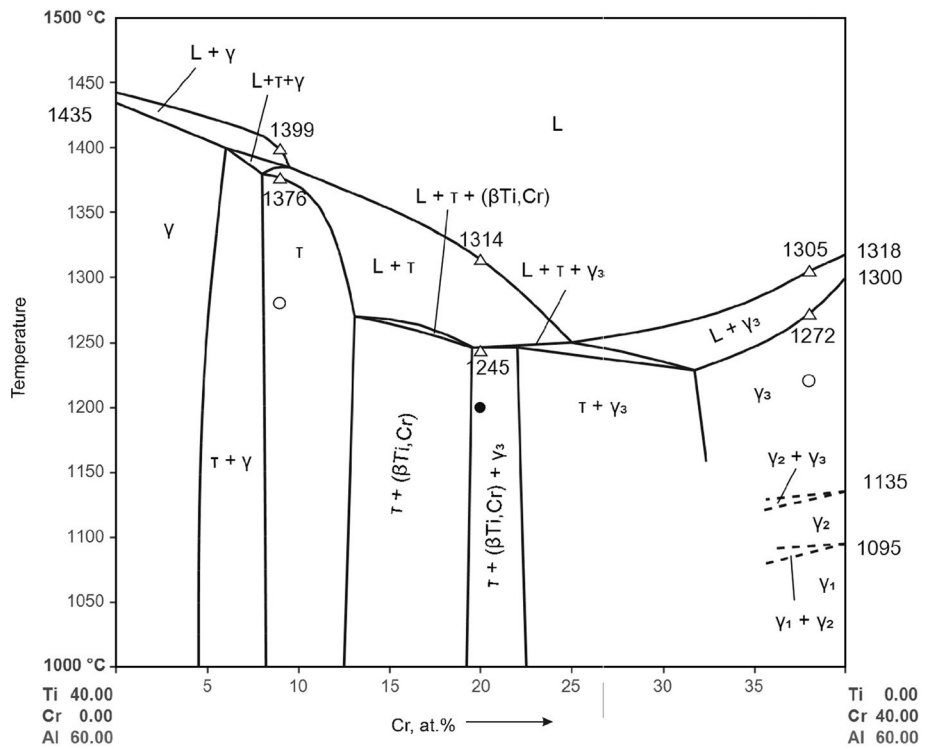
**Fig. 10** Isopleth at 70 at.% Al: half vertical filled circle—two-phase sample; filled circle—three-phase sample; open triangle—DTA data



# References

1. R.W. Hayes, and P.L. Martin, Tension Creep of Wrought Single Phase γTiAl, *Acta Metall. Mater.*, 1995, **43**(7), p 2761-2772. https://doi.org/10.1016/0956-7151(94)00486-2

2. A. Rahmel, W.J. Quadakkers, and M. Schűtze, Fundamentals of TiAl Oxidation—A Critical Review, *Mater. Corros.*, 1995, **46**(5), p 271-285. https://doi.org/10.1002/maco.19950460503

3. C.T. Liu, J.H. Schneibel, P.J. Maziasz, J.L. Wright, and D.S. Easton, Tensile Properties and Fracture Toughness of TiAl Alloys with Controlled Microstructures, *Intermetallics*, 1996, **4**(6), p 429-440. https://doi.org/10.1016/0966-9795(96)00047-7

4. C. Mercer, J. Lou, and W.O. Soboyejo, An Investigation of Fatigue Crack Growth in a Cast Lamellar Ti-48Al-2Cr-2Nb Alloy, *Mater. Sci. Eng. A.*, 2000, **284**(1-2), p 235-245. https://doi.org/10.1016/S0921-5093(00)00702-4

5. M. Yamaguchi, H. Inui, and K. Ito, High-temperature Structural Intermetallics, *Acta Mater.*, 2000, **48**(1), p 307-322. https://doi.org/10.1016/S1359-6454(99)00301-8

6. W.J. Zhang, and S.C. Deevi, The Controlling Factors in Primary Creep of TiAl-Base Alloys, *Intermetallics*, 2003, **11**(2), p 177-185. https://doi.org/10.1016/S0966-9795(02)00226-1

7. F. Appel, An Electron Microscope Study of Mechanical Twinning and Fracture in TiAl Alloys, *Philos. Mag.*, 2005, **85**(2-3), p 205-231. https://doi.org/10.1080/14786430412331315662

8. W.O. Soboyejo, and C. Mercer, On the Influence of Thermo-mechanical Processing on the Fracture Behavior of Gamma-Based Titanium Aluminides II. Effects of Alloying with Cr and Nb, *Mater. Manuf. Processes*, 1996, **11**(3), p 431-448. https://doi.org/10.1080/10426919608947495

9. L.J. Parfitt, J.L. Smialek, J.P. Nic, and D.E. Mikkola, Oxidation Behavior of Cubic Phases Formed by Alloying Al₃Ti with Cr and Mn, *Scr. Metall. Mater.*, 1991, **25**(3), p 727-731. https://doi.org/10.1016/0956-716X(91)90123-I

10. D.B. Lee, S.H. Kim, K. Niinobe, C.W. Yang, and M. Nakamura, Effect of Cr on the High Temperature Oxidation of L1₂–type Al₃Ti Intermetallics, *Mater. Sci. Eng. A.*, 2000, **290**(1–2), p 1–5. https://doi.org/10.1016/S0921-5093(00)00956-4

11. J.K. Lee, M.W. Oh, M.H. Oh, and D.M. Wee, Phase Stability of L1₂-Based Alloys in Al-Ti-Cr Systems, *Intermetallics*, 2003, **11**(8), p 857-865. https://doi.org/10.1016/S0966-9795(03)00084-0

12. J.H. Choi, and D.B. Lee, High Temperature Corrosion of Al₃Ti-Cr Intermetallics in SO₂ Atmosphere, *Adv. Mat. Res.*, 2007, **398**(15-17), p 398-403. https://doi.org/10.4028/www.scientific.net/AMR.15-17.398

13. I.I. Kornilov, V.S. Mikheev, and T.S. Chernova, Investigations of Phase Diagram of the Ti-Cr-Al System, *Zh. Neorg. Khim.*, 1958, **3**(3), p 786-796 **(in Russian)**

14. T.J. Jewett, B. Ahrens, and M. Dahms, Stability of TiAl in the Ti-Al-Cr System, *Mater. Sci. Eng. A.*, 1997, **225**(1-2), p 29-37. https://doi.org/10.1016/S0921-5093(96)10841-8

15. H. Mabuchi, H. Tsuda, T. Matsui, and K. Morii, Microstructure and Mechanical Properties of Ternary L1₂ Intermetallic Compound in Al-Ti-Cr System, *Mater. Trans. JIM.*, 1997, **38**(6), p 560-565.

16. G. Shao, and P. Tsakiropoulos, Solidification Structures of Ti-Al-Cr Alloys, *Intermetallics*, 2003, **7**(5), p 579-587. https://doi.org/10.1016/S0966-9795(98)00067-3

17. M. Ichimaru, N. Mori, and Y. Miura, Al-Ti-Cr Ternary Phase Diagram and Solidification Structure of (Al, Cr)₃Ti Alloys, *J. JILM.*, 2001, **51**(12), p 640-645.

18. O.M. Barabash, Yu.V. Milman, D.V. Miracle, M.V. Karpets, N.P. Korzhova, T.N. Legkaya, N.M. Mordovets, Yu.N. Podrezov, and I.V. Voskoboinik, Formation of Periodic Microstructures Involving the L1₂ Phase in Eutectic Al-Ti-Cr Alloys, *Intermetallics*, 2003, **11**(9), p 953-962. https://doi.org/10.1016/S0966-9795(03)00122-5

446

J. Phase Equilib. Diffus. (2022) 43:427–447

19. N. Mori, and K. Ogi, Solidification-Path and Microstructure of Al-Ti-Cr Alloy Analyzed by Progressive-Type Solidification Equation, *Mater. Trans. JIM.*, 2003, **44**(11), p 2334-2338.

20. H. Chen, F. Weitzer, N. Krendelsberger, Y. Du, and J. Schuster, Reaction Scheme and Liquidus Surface of the Ternary System Aluminum–Chromium–Titanium, *Metall. Mater. Trans. A*, 2009, **40A**(12), p 2980-2986. https://doi.org/10.1007/s11661-009-0014-z

21. Yu.I. Rusnyak, E.F. Kazakova, and T.P. Loboda, Phase Equilibria in the Al-Cr-Ti System, *Met. Sci. Heat Treat.*, 2009, **51**(9-10), p 433-435. https://doi.org/10.1007/s11041-010-9187-8

22. F.H. Hayes, The Al-Cr-Ti System (Aluminum–Chromium–Titanium), *J. Phase Equilib.*, 1992, **13**(1), p 79-86. https://doi.org/10.1007/BF02645384

23. V. Raghavan, Al-Cr-Ti (Aluminum–Chromium–Titanium), *J. Phase Equilib. Diff.*, 2005, **26**(4), p 349-356. https://doi.org/10.1361/154770305X56809

24. V. Raghavan, Al-Cr-Ti (Aluminum–Chromium–Titanium), *J. Phase Equilib. Diff.*, 2010, **31**(6), p 548-549. https://doi.org/10.1007/s11669-010-9768-7

25. V. Raghavan, Al-Cr-Ti (Aluminum–Chromium–Titanium), *J. Phase Equilib. Diff.*, 2012, **33**(2), p 137-139. https://doi.org/10.1007/s11669-012-0011-6

26. N. Bochvar, T. Dobatkina, O. Fabrichnaya, V. Ivanchenko, D. Cupid, in *Aluminium–Chromium–Titanium, Ternary Alloy Systems, Phase Diagrams, Crystallographic and Thermodynamic Data, Landolt-Boernstein, Numerical Data and Functional Relationships in Science and Technology*, ed. by W. Martienssen. (Springer-Verlag, Berlin-Heidelberg, 2008). IV/11E1, p 24-32. https://doi.org/10.1007/978-3-540-88053-0_7

27. L.-Y. Chen, A.-T. Qiu, L.-J. Liu, M. Jiang, X.-G. Lu, and C.-H. Li, Thermodynamic Modeling of the Ti-Al-Cr System, *J. Alloys Compd.*, 2011, **509**, p 1936-1946. https://doi.org/10.1016/j.jallcom.2010.10.092

28. D.M. Cupid, M.J. Kriegel, O. Fabrichnaya, F. Ebrahimi, and H.J. Seifert, Thermodynamic Assessment of the Cr-Ti and First Assessment of the Al-Cr-Ti Systems, *Intermetallics*, 2011, **19**(8), p 1222-1235. https://doi.org/10.1016/j.intermet.2011.03.031

29. X.G. Lu, C.H. Li, L.Y. Chen, A.T. Qiu, and W.Z. Ding, Calculation of Phase Equilibria in Ti-Al-Cr-Mn Quaternary System for Developing Lower Cost Titanium Alloys, *Mater. Chem. Phys.*, 2011, **129**(3), p 718-728. https://doi.org/10.1016/j.matchemphys.2011.04.017

30. H. Wang, N. Warnken, and R.C. Reed, Thermodynamic Assessment of the Ordered B2 Phase in the Ti-V-Cr-Al Quaternary System, *Calphad*, 2011, **35**(2), p 204-208. https://doi.org/10.1016/j.calphad.2011.02.005

31. M.J. Kriegel, D. Pavlyuchkov, D. Chmelik, O. Fabrichnaya, K. Korniyenko, D. Heger, D. Rafaja, and H.J. Seifert, Constitution of the Liquidus and Solidus Surfaces of the Al-Ti-Cr System, *J. Alloys Compd.*, 2014, **584**, p 438-446. https://doi.org/10.1016/j.jallcom.2013.09.067

32. V.T. Witusiewicz, A.A. Bondar, U. Hecht, and T.Y. Velikanova, Thermodynamic Re-Modelling of the Ternary Al-Cr-Ti System with Refined Al-Cr Description, *J. Alloys Compd.*, 2015, **644**, p 939-958. https://doi.org/10.1016/j.jallcom.2015.04.231

33. V.T. Witusiewicz, A.A. Bondar, U. Hecht, S. Rex, and T.. Ya.. Velikanova, The Al-B-Nb-Ti System: III. Thermodynamic Re–Evaluation of the Constituent Binary System Al-Ti, *J. Alloys Compd.*, 2008, **465**(1-2), p 64-77. https://doi.org/10.1016/j.jallcom.2007.10.061

34. G. Kurtuldu, P. Jessner, and M. Rappaz, Peritectic Reaction on the Al-rich Side of Al-Cr System, *J. Alloys Compd.*, 2015, **621**, p 283-286. https://doi.org/10.1016/j.jallcom.2014.09.174

35. S. Cui, I.-H. Jung, J. Kim, and J. Xin, A Coupled Experimental and Thermodynamic Study of the Al-Cr and Al-Cr-Mg Systems, *J. Alloys Compd.*, 2017, **698**, p 1038-1057. https://doi.org/10.1016/j.jallcom.2016.12.298

36. F. Stein, M. Palm, and G. Sauthoff, Structure and Stability of Laves Phases Part II—Structure Type Variations in Binary and Ternary Systems, *Intermetallics*, 2005, **13**(10), p 1056-1074. https://doi.org/10.1016/j.intermet.2004.11.001

37. P.A. Farrar, and H. Margolin, A Reinvestigation of Chromium-Rich Region of the Titanium-Chromium System, *Trans. Met. Soc. AIME*, 1963, **227**, p 1342-1345.

38. K.C. Chen, S.M. Allen, and J.D. Livingston, Stoichiometry and Alloying Effects on the Phase Stability and Mechanical Properties of TiCr₂-base Laves Phases, *Mat. Res. Soc. Symp. Proc.*, 1995, **364**, p 1401-1406. https://doi.org/10.1557/PROC-364-1401

39. S.A. Minaeva, P.B. Budberg, and A.L. Gavze, Phase Structure of Ti-Cr Alloys, *Izv. Akad. Nauk SSSR. Met.*, 1971, **4**, p 205-209, (**in Russian**)

40. T.B. Massalski, Ed., *Binary Alloy Phase Diagrams* 2'nd edn ASM International, Ohio, 1990

41. J. Braun, and M. Ellner, Phase Equilibria Investigations on the Aluminium-Rich Part of the Binary System Ti-Al, *Metall. Mater. Trans. A*, 2001, **32A**(5), p 1037-1048. https://doi.org/10.1007/s11661-001-0114-x

42. J.C. Schuster, and H. Ipser, Phases and Phase Relations in the Partial System TiAl₃-TiAl, *Z. Metallkd.*, 1990, **81**(6), p 389-396.

43. M.J. Blackburn, The Ordering Transformation in Titanium: Aluminum Alloys Containing up to 25 at. pct Al, *Trans. Met. Soc. AIME*, 1967, **239**(8), p 1200-1208.

44. M.J. Cooper, The Structure of the Intermetallic Phase θ (Cr-Al), *Acta Cryst.*, 1960, **13**(3), p 257-263. https://doi.org/10.1107/S0365110X60000571

45. T. Ohnishi, Y. Nakatani, and K. Okabayashi, Crystal Structures of Intermetallic θ, η and ε Phases in Cr-Al System, *Bull Univ. Osaka Prefect. Ser. A. Eng. Nat. Sci.*, 1976, **24**(2), p 183-191. https://doi.org/10.24729/00008713

46. L.A. Bendersky, R.S. Roth, J.T. Ramon, and S. Shechtman, Crystallographic Characterization of Some Intermetallic Compounds in the Al-Cr System, *Metall. Trans. A*, 1991, **22**(1), p 5-10. https://doi.org/10.1007/BF03350943

47. M. Audier, M. Durand-Charre, E. Laclau, and H. Klein, Phase Equilibria in the Al-Cr System, *J. Alloys Compd.*, 1995, **220**, p 225-230. https://doi.org/10.1016/0925-8388(94)06010-X

48. B. Grushko, B. Przepiorzynski, E. Kowalska-Strzeciwilk, and M. Surowiec, New Phase in the High-Al Region of Al-Cr, *J. Alloys Compd.*, 2006, **420**, p L1-L4. https://doi.org/10.1016/j.jallcom.2005.10.0465

49. J. Braun, M. Ellner, and B. Predel, Zur Struktur der Hochtemperaturphase Cr₅Al₈ (h), *J. Alloys Compd.*, 1992, **183**, p 444-448. https://doi.org/10.1016/0925-8388(92)90766-3

50. J.W. Visser, On the Structure of (Cr₅Al₈) 26R, *Acta Cryst. B.*, 1977, **33**, p 316. https://doi.org/10.1107/S0567740877003549

51. M. Ellner, J. Braun, and B. Predel, Röntgenographische Untersuchung an Cr-Al-Phasen der W-Familie, *Z. Metallkd.*, 1989, **80**(5), p 374-383.

52. I. Jacob, A. Stern, A. Moran, D. Shaltiel, and D. Davidov, Hydrogen Absorption in (Zr$_x$Ti$_{1-x}$)B₂ (B ≡ Cr, Mn) and the Phenomenological Model for the Absorption Capacity in Pseudo-Binary Laves-phase Compounds, *J. Less-Common Met.*, 1980, **73**(2), p 369-376. https://doi.org/10.1016/0022-5088(80)90331-8

53. B. Prasad, X-Ray Diffraction Study of Imperfections in the Laves Phase TiCr₂, *Phys. Stat. Sol. (A)*, 1973, **19**(1), p K97-K100. https://doi.org/10.1002/pssa.2210190164

54. I. Jacob, and D. Shaltiel, A Note on the Influence of Al on the Hydrogen Sorption Properties of Ti(Al$_x$B$_{1-x}$)₂ (B = Cr, Mn, Fe, Co), *Mat. Res. Bull.*, 1978, **13**(11), p 1193-1198. https://doi.org/10.1016/0025-5408(78)90208-8

J. Phase Equilib. Diffus. (2022) 43:427–447

447

55. C.J. Sparks, W.D. Porter, J.H. Schneibel, W.C. Oliver, and C.G. Golec, Formation of Cubic L1$_2$ Phases from Al$_3$Ti and Al$_3$Zr by Transition Metal Substitutions for Al, *Mat. Res. Soc. Symp. Proc.*, 1991, **186**, p 175-180. https://doi.org/10.1557/PROC-186-175

56. Ju.A. Kocherzhinsky, Differential Thermocouple up to 2450 °C and Thermographic Investigations of Refractory Silicides, in *Proc. 3rd ICTA (Davos)*, (Birkhäuser Verlag, Basel, 1971), **1**, p 549-559

57. Ju.A. Kocherzhinsky, Ye.A. Shishkin and V.I. Vasilenko, Apparatus for Differential Thermal Analysis with Temperature-Sensing Thermocouple up to 2200 °C. eds. N.V. Ageev and O.S. Ivanov *Diagrammy Sostoyaniya Metallicheskikh Sistem*, (Moscow, Nauka, 1971), p 245-249, (**in Russian**)

58. M.J. Kriegel, D. Pavlyuchkov, D.M. Cupid, O. Fabrichnaya, D. Heger, D. Rafaja, and H.J. Seifert, Phase Equilibria at 1473 K in the Ternary Al-Ti-Cr System, *J. Alloys Compd.*, 2013, **550**, p 519-525. https://doi.org/10.1016/j.jallcom.2012.10.123